Lepton Flavour Violation in Supersymmetry

A thesis submitted towards partial fulfilment of
BS-MS Dual Degree Programme

by

UTKARSH GIRI

under the guidance of

PROF. ROHINI GODBOLE
and
PROF. SUDHIR VEMPATI

CENTRE FOR HIGH ENERGY PHYSICS, IISc

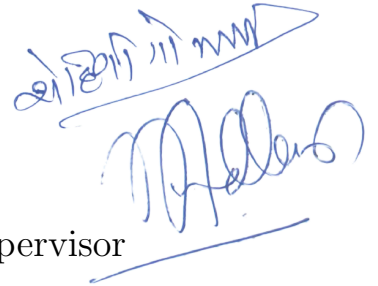INDIAN INSTITUTE OF SCIENCE EDUCATION AND RESEARCH PUNE

Certificate

This is to certify that this thesis entitled "Lepton Flavour Violation in Supersymmetry" submitted towards the partial fulfilment of the BS-MS dual degree programme at the Indian Institute of Science Education and Research Pune represents original research carried out by Utkarsh Giri at Centre for High Energy Physics, Indian Institute of Science, under the joint supervision of Prof. Rohini Godbole and Prof. Sudhir Vempati during the academic year 2014-2015.

Student
UTKARSH GIRI

Supervisor
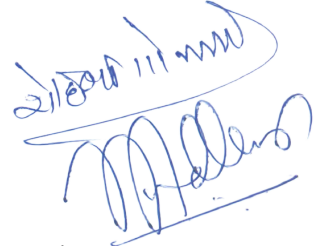ROHINI GODBOLE
and
SUDHIR VEMPATI

Declaration

I hereby declare that the matter embodied in the report entitled "Lepton Flavour Violation in Supersymmetry" are the results of the investigations carried out by me at the Centre of High Energy Physics, Indian Institute of Science, under the joint supervision of Prof. Rohini Godbole and Prof. Sudhir Vempati and the same has not been submitted elsewhere for any other degree.

Student

UTKARSH GIRI

Supervisor

ROHINI GODBOLE

and

SUDHIR VEMPATI

Acknowledgements

Abstract

Supersymmetry is one of the most popular and highly motivated theories beyond the Standard Model. Apart from providing a solution to the hierarchy problem, it also leads to unification of couplings at high energies and has a candidate particle for dark matter. The Large Hadron Collider (LHC) has looked for supersymmetric particles in their searches with no success till date. The collider is set to restart colliding particles again in 2015 at an upgraded energy scale of 13 TeV. The entire particle physics fraternity is hopeful of observing first signs of supersymmetric particle in the coming years. Once the particles are detected, the next step for the experimentalists would be to obtain the properties of these particles, for instance their masses and mixing.

One of the features of interest is Lepton Flavour Violation (LFV). Lepton flavour is inherently conserved in the Standard Model owing to the massless nature of neutrinos. Supersymmetry in its general form does not require generational lepton number conservation. However, the null results in various experiments looking for LFV decays has put strong constraints on the possibility of flavour violation in supersymmetric models. Notwithstanding these constraints, the possibility of flavour violation in the decay of supersymmetric particles is not completely ruled out. In fact under certain conditions, significant LFV could be possible.

In this study, we have calculated the constraints on slepton (supersymmetric lepton) mass matrix coming from rare decays of electron, muon and tau. Based on these results, we obtain the condition for substantial flavour violation. Next we study a signal for lepton flavour violating decay of a supersymmetric particle neutralino, which can be investigated at the LHC.

Contents

Chapter 1

Introduction

1.1 Lepton Flavour Violation in Standard Model

In the Standard Model, both the up and down quarks of all the three generations are massive with non-degenerate masses generated via spontaneous symmetry breaking . In the mass eigenstate of up-type quarks, the Wu_id_j vertex where u_i are the up-type quark fields u, c and t while d_i are down-type quark fields d, s and b, is not a diagonal matrix in the generation space. Consequently, the quark mass eigenstates are different from their flavour (gauge) eigenstate and can be represented as superposition of the three flavour eigenstates. In other words, baryon flavour number is not strictly conserved in SM.

The situation is completely different in the leptonic sector. Since the neutrinos are massless and hence degenerate, $Wl_i\nu_j$ vertex, where $l_i = e, \mu, \tau$ are charged leptons and $\nu_j = \nu_e, \nu_\mu, \nu_\tau$ are the corresponding neutrinos, is diagonal in the generation space in the basis of mass eigenstates for charged leptons and neutrinos. As a result, the neutrinos do not mix and the family lepton number is conserved in SM.

In the 1990's, experiments designed to measure the solar neutrino flux on earth found that the flux was not consistent with the theoretical prediction[1]. The results pointed towards oscillation of neutrinos into one another which could only be possible if they had non-degenerate masses. By 1998, the result from Super Kamiokande experiment[2] established beyond reasonable doubt that neutrinos were massive and undergo oscillations.

The fact that neutrinos have masses and undergo oscillation has huge implication for the lepton sector of the Standard Model. Under the scenario where neutrinos are massive and oscillating, processes such as $\mu \to e\gamma, \tau \to \mu\gamma$ which are forbidden in the Standard Model, can now take place via an oscillating neutrino in the internal leg of one loop feynman diagram.

The decay width for $\mu \to e\gamma$ is given by[3]

$$\Gamma(\mu \to e\gamma) = \frac{m_\mu}{8\pi}(|A_L|^2 + |A_R|^2) \tag{1.1}$$
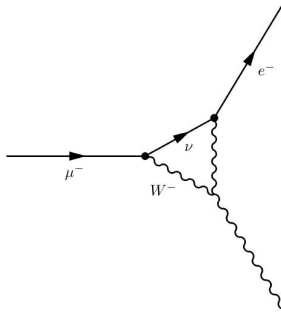
Figure 1.1: The decay of muon to electron through W exchange

where A_L and A_R are the invariant amplitudes for left handed and right handed electron, respectively. In the limit where electron mass goes to 0, we have

$$A_R = 0$$

$$A_L = e\frac{g^2}{4M_W^2}\frac{m_\mu}{32\pi^2}\delta_\nu \tag{1.2}$$

where δ_ν is given by

$$\delta_\nu = \frac{\sum_i U_{ei}^* U_{\mu i} m_i^2}{M_W^2} \tag{1.3}$$

and the branching fraction is

$$Br(\mu \to e\gamma) = \frac{3\alpha}{32\pi}\delta_\nu^2 \tag{1.4}$$

which is highly suppressed ($< 10^{-50}$) owing to the vanishingly small mass of neutrinos. The sensitivity of experiments probing the lepton flavour violating decays is too small to detect such small values of branching fraction and no flavour violation has ever been observed in any experiment. The null results have been used to set limits on rare decays 1.1. Thus any flavour violation occuring solely due to the massiveness of neutrinos will remain beyond experimental reach for a long time. This may look discouraging but it is actually a boon.

Experimental Limits on rare decay	
$Br(\mu \to e\gamma)$	5.7×10^{-13} [4]
$Br(\tau \to \mu\gamma)$	4.4×10^{-8} [5]
$Br(\tau \to e\gamma)$	3.3×10^{-8} [5]

Table 1.1: Constraints on Branching Fraction of rare decay

Consider eq. (1.4), suppose in place of light neutrinos, we had particles with mass of $\mathcal{O}(1)$ TeV in the internal leg with an identical mixing matrix U along with equally

massive exchange particle. We would then get an $\mathcal{O}(10^{36})$ increase in the LFV decay rate which will bring it into the detectable range. However there is no known particle upto the weak scale which can replace neutrinos in the above feynman diagram. The fact that the rare decay branching ratio's are non-detectable under Standard Model with massive neutrino implies that if upcoming experiments were to detect a non zero branching ratio, it would be a definite sign of physics above weak scale. Consequently one would be able to probe higher enrgy physics through these decays.

However, if the higher physics scale is characterised by an energy scale Λ, then Λ appears with a negative power in the effective lagrangian for $\mathrm{Br}(\mu \to e\gamma)$ which is a dimesion five operator

$$\frac{1}{\Lambda}\bar{\psi}\sigma^{\mu\nu}(A + B\gamma_5)\psi F_{\mu\nu} \tag{1.5}$$

If the new physics enters at around Planck scale ($\sim 10^{18}$ GeV) then again the flavour violating amplitude will be suppressed due to the presence of Λ in the denominator irrespective of the nature of mixing matrix [6].

Therefore, it follows that the best hope for probing high energy physics through rare decays would be if the new physics exists not much above the weak scale. Fortunately, supersymmetry, one of the possible extensions of the Standard Model is motivated to be realized just above the weak scale.

1.2 A Caveat: Flavour Problem

The fact that rare decays are extremely suppresed in the SM with massive neutrinos is because of the huge gap in the order of magnitude of neutrino masses and W-boson. If supersymmetry is an answer to the hierarchy problem, then we should have $\Lambda_{SUSY} \sim \mathcal{O}(1)$ TeV. The negative results for SUSY searches have put lower bounds on the masses of SUSY particles. The upshot is that SUSY not only allows large lepton flavour violation but in fact the generic prediction will be far above the observed low rates for these LFV processes. Two solutions exist.

If the lepton and slepton mass matrices are proportional to each other (called alignment), then δ_ν will vanish altogether and the problem will be solved [7]. But such a choice of mass matrix has to be justified. Another way out is if the sleptons are degenerate. Then, just like in case of degenerate neutrinos of SM [3] there would not be any LFV. Here again, the slepton degeneracy has to be motivated and justified.

1.3 Lepton Flavour Violation at LHC

A lepton and its superpartner slepton have the same family lepton number. Under family lepton conservation, the number should be conserved in a process. However,

owing to this misalignment of slepton mass matrix, in the mass eigenstate of lepton and neutralino/chargino, the slepton mass states are not diagonal. As a result it is possible to have decays like

$$\widetilde{\ell}_j \to \ell_i \widetilde{\chi}_1^0 \tag{1.6}$$

$$\widetilde{\nu}_j \to \nu_i \widetilde{\chi}_1^0 \tag{1.7}$$

where i, j are flavour indices. Although the neutrinos produced in the sneutrino decay leave the detector undetected, the slepton decay into a lepton of different flavour can be, in principle, observed at colliders, thus providing us with an opportunity to probe LFV at a collider.

Chapter 2

Supersymmetry

2.1 Introduction

The Standard Model of particle physics can successfully account for the properties of and interactions among the fundamental particles upto TeV energy scales to a very high precision ($\sim$1 part in 10^3 for EW physics). However, the Standard Model still can not be considered as a complete theory of nature. The model totally ignores gravity which is one of the four fundamental forces of nature. Moreover in the last couple of decades, it has been established that matter, as we know it, only constitutes a tiny fraction of the universe. The universe is dominated by two mysterious entities, called Dark Energy and Dark Matter, which are yet to be understood and explained. The Standard Model which originated out of various theoretical and experimental endeavours, way back in the 1970's, does not explain these two aspects of nature. It has no explanation for matter-antimatter asymmetry and neutrino oscillations either.

Supersymmetry is an extension of the Standard Model which postulates a symmetry between fermions (spin half particle) and bosons (integer spin particle). A supersymmetric operator transforms a fermionic field into bosonic one and vice versa.

$$\mathcal{Q} \left| Boson \right\rangle = \left| Fermion \right\rangle \tag{2.1}$$

$$\mathcal{Q} \left| Fermion \right\rangle = \left| Boson \right\rangle \tag{2.2}$$

The theory predicts existence of a partner particle (called superparticle) for each particle of the standard model which differ from each other by spin half and are related by supersymmetric transformation. Since the theory is an extension of the highly successful Standard Model, it must preserve the Lorentz and gauge symmetry of the SM and must also be renormalizable and anomaly free. For the next section, we follow the analysis and notation of [7, 10, 11]

2.2 Motivation

2.2.1 The Hierarchy problem

Within the Standard Model, although the masses of fermion and gauge bosons are protected by chiral symmetry and gauge symmetry respectively, there is no symmetry to protect Higgs mass. The higgs mass receives large corrections from loop involving the heavy top quarks which drives it to extremely high values. Under the assumption of no new physics upto Planck scale, the large corrections to the mass can be avoided by fine-tuning the parameters to an order of one part in 10^{36}. [11] However such contrived choice of parameter is deemed unnatural and unjustified and is not believed to be the actual solution to the problem . Supersymmetry provides an ingenious solution to the problem [10]. The leading coreection Δm_h^2 from a fermionic loop of a fermion f with coupling λ_f is

$$\Delta m_h^2 = -\frac{|\lambda_f|^2}{8\pi^2}\Lambda_{\text{cutoff}}^2 + \dots \tag{2.3}$$

The contribution from a scalar particle with coupling λ_s comes out to be

$$\Delta m_h^2 = \frac{|\lambda_S|}{16\pi^2}\Lambda_{\text{cutoff}}^2 + \dots \tag{2.4}$$

where Λ_{cutoff} is cutoff scale. If for each fermion, we have two scalar particles, with $\lambda_S = |\lambda_f|^2$, then the leading quadratic correction from the fermions and bosons exactly cancel out!. We will come back to it in the next section.

Figure 2.1: One loop diagram which give fermionic and bosonic correction to Higgs mass..

2.2.2 Coupling Unification

When the gauge couplings of $SU(3)_C \times SU(2)_L \times U(1)_Y$ gauge group of the standard model are evolved to high energy scales through renormalization group equation, they don't quite meet at a common point of energy scale. However the supersymmetric evolution appears to give a unique point where all the couplings converge.
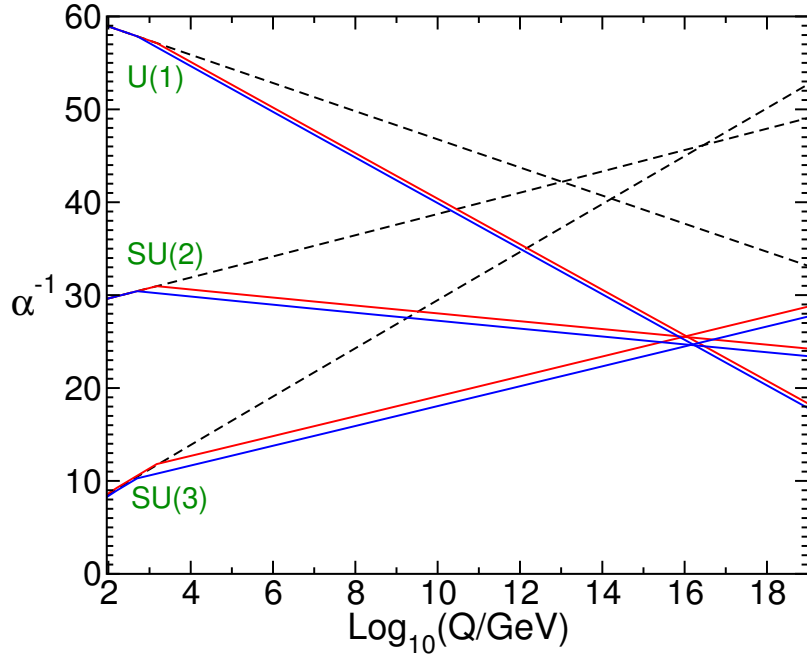
Figure 2.2: Two loop RG evolution of coupling constants in SM and SUSY. The dashed lines are from SM while the coloured solid are from SUSY. The figure is taken from Ref [10]

2.2.3 Dark Matter Candidate

Dark matter is believed to compose 26.8% of the Universe [12]. However the identity of dark matter (DM) still elludes us. A Weakly Interacting Massive particle (WIMP) having a mass of around 100 GeV is hypothesized to be a major, if not the only constituent of DM [13]. Supersymmetry under the assumption of R-parity[1] conservation gives a candidate WIMP.

2.2.4 Gravity

When the supersymmetry is elevated from a global symmetry to a local symmetry dependent on space-time variable x^μ, then under infinitesimal transformation of the lagrangian, extra fermionic terms are generated which spoil the symmetry if not taken care of. To regain the symmetry, one needs to introduce a fermionic field with a spin of 3/2 . This spin 3/2 particle is identified as the superpartner of graviton, the particle which mediates gravity. The model thus naturally incorporates gravity, the only interaction missing from the Standard Model.

---

[1] To avoid terms which violate baryon and lepton number conservetion in the lagrangian, one imposes the condition that the lagrangian terms must be invariant under R-parity where the superfields transform as

$$\mathcal{R}_\mathcal{P} = (-1)^{3(B-L)2s} \tag{2.5}$$

2.3 Minimal Supersymmetric Standard Model (MSSM)

MSSM is Minimal Supersymmetric Standard Model. This is an extension of SM with minimum number of particles needed to incorporate a self consistent SUSY.

In supersymmetry, the analogues of quantum field of SM are called superfields or super-multiplet which are function over superspace which is an eight dimensional space with 4 space-time and 4 fermionic degrees of freedom. The gauge group of MSSM, like SM , is $SU(3)_C \times SU(2)_L \times U(1)_Y$. The particle content and their respective gauge transformations are given in Table   The superfields come in two forms; chiral supermultiplets containing left chiral fermions and vector supermultiplets containg vector bosons of SM, in additon to their respective superparticle fields and auxillary field[2] The particle spectrum of the MSSM and their transformation properties under the $SU(3)_C \times SU(2)_L \times U(1)_Y$ gauge group is given by,

$$Q_i \equiv \begin{pmatrix} u_{L_i} & \tilde{u}_{L_i} \\ d_{L_i} & \tilde{d}_{L_i} \end{pmatrix} \sim \left(3,\ 2,\ \frac{1}{6} \right) \qquad U_i^c \equiv \begin{pmatrix} u_i^c & \tilde{u}_i^c \end{pmatrix} \sim \left(\bar{3},\ 1,\ -\frac{2}{3} \right)$$

$$D_i \equiv \begin{pmatrix} d_i^c & \tilde{d}_i^c \end{pmatrix} \sim \left(\bar{3},\ 1,\ \frac{1}{3} \right)$$

$$L_i \equiv \begin{pmatrix} L_i & \tilde{L}_i \\ e_{L_i} & \tilde{e}_{L_i} \end{pmatrix} \sim \left(1,\ 2,\ -\frac{1}{2} \right) \qquad E_i \equiv \begin{pmatrix} e_i^c & \tilde{e}_i^c \end{pmatrix} \sim (1,\ 1,\ 1)$$

The supersymmetric lagrangian is constructed from these superfields. The part of the lagrangian which gives kinetic term for SM fermion and sfermions and their interaction with gauge boson is given by

$$\mathcal{L}_{kin} = \int d\theta^2 d\bar{\theta}^2 \sum \Phi_\beta^\dagger e^{gV} \Phi_\beta \tag{2.8}$$

where β runs over all the chiral superfields while the summation is over the vector superfields.

---

[2]. A chiral superfield can be written as

$$\Phi = \phi + \sqrt{2}\theta.\chi + \theta.\theta F \tag{2.6}$$

where χ is the left chiral SM fermion while ϕ is its scalar superpartner. F is an auxillary field introduced to keep supersymmetry intact even 'off-shell'.
A vector superfield in Wess-Zumino gauge can be expressed as

$$V = -\theta\sigma^\mu\bar{\theta}A_\mu + i\theta\theta\bar{\theta}\bar{\lambda} - i\bar{\theta}\bar{\theta}\theta\lambda + \frac{1}{2}\theta\theta\bar{\theta}\bar{\theta}D \tag{2.7}$$

where A_μ is a SM gauge field while λ is its supersymmetric fermionic partner. D here is the auxillary field.

The counterparts of yukawa terms in SM come from

$$\mathcal{L}_{yuk} = \int d\theta^2 W(\Phi) + h.c. \tag{2.9}$$

where W is an analytic function of superfields called the superpotential and is given by

$$W = W_1 + W_2 \tag{2.10}$$

where

$$W_1 = h_{ij}^u Q_i U_j^c H_2 + h_{ij}^d Q_i D_j^c H_1 + h_{ij}^e L_i E_j^c H_1 + \mu H_1 H_2 \tag{2.11}$$

$$W_2 = \epsilon_i L_i H_2 + \lambda_{ijk} L_i L_j E_k^c + \lambda'_{ijk} L_i Q_j D_k^c + \lambda_{ijk} U_i^c D_j^c D_k^c \tag{2.12}$$

Under the assumption of R-parity, the W_2 part vanishes. The gauge part of the lagrangian is written as

$$\mathcal{L}_g = \int d\theta^2 \mathcal{W}^\alpha \mathcal{W}_\alpha + h.c. \tag{2.13}$$

where $\mathcal{W}^\alpha$ are field strength superfield constructed from respective vector superfields and α runs over all the vector superfields. To sum things together, MSSM lagrangian under exact supersymmetry is given by

$$\mathcal{L}_{SUSY} = \mathcal{L}_{kin} + \mathcal{L}_{yuk} + \mathcal{L}_g \tag{2.14}$$

2.3.1   A Broken Symmetry

If supersymmetry were an exact symmetry of nature we would expect SUSY particles to have masses identical to their corresponding SM particle. However since no such particle has been observed in nature, SUSY must be a broken symmetry. The manner of SUSY breaking has been a matter of speculation. A supersymmetry breaking at weak scale would imply existence of SUSY particle with masses less than SM particles. Since this has not been observed, supersymmetry breaking at weak scale is ruled out. Since SSB is much desired, models have been postulated with SSB enforced at high energies like Minimal Supergravity and Anomaly Mediated Spontaneous Breaking. However irrespective of the mechanism, the symmetry breaking at weak scale can be parametrized in terms of explicit soft terms.

Coming back to the hierarchy problem, the solution to hierarchy problem from supersymmetry is exact as long as $|\lambda_S| = |\lambda_f^2|$ where λ_S and λ_f are coupling constants from Eq. 2.3 and 2.4. However, since SUSY is broken , the couplings which are related to the particle masses, may not be related in the desired fashion as to cancel out all corrections. Therefore if SUSY has to provide solution to the hierarchy problem, the relationship between coupling constants in the unbroken case must hold while at the same time, the correction

from SUSY breaking terms must be protected by supersymmetry. The Lagrangian, is therefore split in two parts

$$\mathcal{L} = \mathcal{L}_{\text{SUSY}} + \mathcal{L}_{\text{soft}} \tag{2.15}$$

where $\mathcal{L}_{\text{SUSY}}$ is totally supersymmetric while $\mathcal{L}_{\text{soft}}$ contains explicit SUSY breaking terms. If the mass scale of SUSY $\mathcal{L}_{\text{soft}} = M$, then in the limit $M \to 0$, Δm_H^2 must vanish. This implies that the correction to Higgs mass under broken symmetry can grow logarithmically at best.

$$\Delta m_h^2 = M^2 \left[\frac{\lambda}{16\pi^2} \ln(\Lambda_{\text{UV}}/M) + \dots \right]. \tag{2.16}$$

The requirement that the correction should not be more than the bare mass implies that M itself has to be around a few TeV's.

The explicit soft susy breaking terms are written as:

$$
\begin{aligned}
-\mathcal{L}_{\text{soft}} = \ & \widetilde{q}_{iL}^*(\mathcal{M}_{\widetilde{q}}^2)_{ij}\widetilde{q}_{jL} + \widetilde{u}_{iR}^*(\mathcal{M}_{\widetilde{u}}^2)_{ij}\widetilde{u}_{jR} + \widetilde{d}_{iR}^*(\mathcal{M}_{\widetilde{d}}^2)_{ij}\widetilde{d}_{jR} + \widetilde{l}_{iL}^*(\mathcal{M}_{\widetilde{l}}^2)_{ij}\widetilde{l}_{jL} \\
& \widetilde{e}_{iR}^*(\mathcal{M}_{\widetilde{e}}^2)_{ij}\widetilde{e}_{jR} + [h_1.\widetilde{l}_{iL}(f^e A^e)_{ij}\widetilde{e}_{jR}^* + h_1.\widetilde{q}_{iL}(f^d A^d)_{ij}\widetilde{d}_{jR}^* + \\
& h_2.\widetilde{q}_{iL}(f^u A^u)_{ij}\widetilde{u}_{jR}^* + h.c.] + m_1^2|h_1|^2 + m_2^2|h_2|^2 + (B\mu h_1.h_2 + h.c.) \\
& + \frac{1}{2}(M_1\bar{\widetilde{\lambda}}_0 P_L\widetilde{\lambda}_0 + M_1^*\bar{\widetilde{\lambda}}_0 P_R\widetilde{\lambda}_0) + \frac{1}{2}(M_2\bar{\widetilde{\lambda}}^i P_L\widetilde{\lambda}^i + M_2^*\bar{\widetilde{\lambda}}^i P_R\widetilde{\lambda}^i) \\
& + \frac{1}{2}(M_3\bar{\widetilde{g}}^a P_L\widetilde{g}^a + M_3^*\bar{\widetilde{g}}^a P_R\widetilde{g})
\end{aligned}
\tag{2.17}
$$

In the above expression $M_{1,2,3}$ are gaugino mass parameters corresponding to $U(1)_Y$, $SU(2)_L$ and $SU(3)_C$ gaugino fields while m_1 and m_2 are real Higgs scalar mass parameters for the higgs doublet $h1$ and $h2$ respectively and $h_1.h_2 = \tilde{h}_1^\dagger h_2$ where $\tilde{h}_1 = i\tau_2 h_1^*$ is an SU(2) doublet. $\mathcal{M}_{\widetilde{q},\widetilde{l}}^2$ are the mass matrices for squared left squark and slepton mass. These are 3×3 hermitian matrices in generation space. $\mathcal{M}_{\widetilde{u},\widetilde{d},\widetilde{e}}^2$ are the mass matrices for squared right quark and slepton mass. These too are 3×3 hermitian matrices in generation space. $f^e A^e$, $f^d A^d$ and $f^u A^u$ are coefficient to trilinear terms. The coefficient of Higgs bilinear term has been factored into the product of μ and B, where B has dimensions of mass. These parameters in general are complex which gives us 125 real unknowns. For phenomenomenological studies, handling these many unknown is next to impossible. Several simplyfying assumptions are made, at times motivated by experimental constraints(for instance null results for CP violation beyond Standard Model) to make the model manageable.

After supersymmetry and electroweak symmetry is broken, the different sparticles having common $U(1)_{em}$ quantum number mix together and acquire masses based on the values of the SUSY breaking parameters.

First we consider sleptons. In the flavour (gauge) basis where the flavour eigenstate is $(e_L, \mu_L, \tau_L, e_R, \mu_R, \tau_R) \equiv (l_L, l_R)$, the slepton mass matrix is given by a 6×6 matrix. For this eigenstate, the mass matrix can be written in blocks of 3×3 matrix as

$$- \mathcal{L}_m = \left(\tilde{l}_L^\dagger, \tilde{l}_R^\dagger \right) \begin{pmatrix} m_L^2 & m_{LR}^{2\mathsf{T}} \\ m_{LR}^2 & m_R^2 \end{pmatrix} \begin{pmatrix} \tilde{l}_L \\ \tilde{l}_R \end{pmatrix}, \tag{2.18}$$

where m_L^2 and m_R^2 are 3×3 hermitian matrices and m_{LR}^2 is a 3×3 matrix. These elements are given as,

$$m_{Lij}^2 = \mathcal{M}_{\tilde{l}ij}^2 + (m_{l_i}^2 + m_Z^2 \cos 2\beta(-\frac{1}{2} + \sin^2 \theta_W))\delta_{ij}, \tag{2.19}$$

$$m_{Rij}^2 = \mathcal{M}_{\tilde{e}ij}^2 + (m_{l_i}^2 - m_Z^2 \cos 2\beta \sin^2 \theta_W)\delta_{ij}, \tag{2.20}$$

$$m_{LRij}^2 = (A_l - m_{l_i}\mu \tan \beta)\delta_{ij}, \tag{2.21}$$

For our case, we assume the above mass matrix to be real. This , in general, need not be diagonal and hence can include mixing between different generations. We diagonalize the mass matrix $\mathcal{M}^2$ by a 6×6 real orthogonal matrix U_L as

$$U_L \mathcal{M}^2 U_L^T = \mathcal{M}_\mathcal{D}, \tag{2.22}$$

and we denote its eigenvalues by $m_{\tilde{l}_X}^2$ $(X = 1, \cdots, 6)$. The mass eigenstate is then written as

$$\tilde{l}_X = U_{LX,i}\tilde{l}_{Li} + U_{LX,i+3}\tilde{l}_{Ri}, \qquad (i = 1, \cdots, 3). \tag{2.23}$$

Conversely, we have

$$\tilde{f}_{Li} = U_{L\,iX}^\mathsf{T}\tilde{f}_X = U_{LXi}\tilde{f}_X, \tag{2.24}$$

$$\tilde{f}_{Ri} = U_{L\,i+3,X}^\mathsf{T}\tilde{f}_X = U_{LX,i+3}\tilde{f}_X. \tag{2.25}$$

Since there are no right handed sneutrinos, the situation is a little simpler here. The sneutrino mass matrix is a 3×3 matrix given by

$$m_{ij}^2 = \mathcal{M}_{\tilde{l}ij}^2 + \left(\frac{1}{2}M_Z^2 \cos 2\beta \right) \delta_{ij}, \tag{2.26}$$

for the basis given by $(\nu_{eL}, \nu_{\mu L}, \nu_{\tau L})$. The diagonalization protocol for neutrino mass matrix is similar to that of slepton mass matrix.

Coming to the case of charginos, we follow the nomenclature of Ref [14] for later convenience. The mass matrix is given by

$$- \mathcal{L}_m = \left(\overline{\tilde{W}_R^-} \; \overline{\tilde{H}_{2R}^-} \right) \begin{pmatrix} M_2 & \sqrt{2}m_W \cos \beta \\ \sqrt{2}m_W \sin \beta & \mu \end{pmatrix} \begin{pmatrix} \tilde{W}_L^- \\ \tilde{H}_{1L}^- \end{pmatrix} + h.c.. \tag{2.27}$$

13

This matrix $\mathcal{M}_\mathcal{C}$ is diagonalized by a 2×2 real orthogonal matrices O_L and O_R as

$$O_R \mathcal{M}_\mathcal{C} O_L^\mathsf{T} = \mathcal{M}_\mathcal{C}^\mathcal{D}. \tag{2.28}$$

If we write

$$\begin{pmatrix} \tilde{\chi}_{1L}^- \\ \tilde{\chi}_{2L}^- \end{pmatrix} = O_L \begin{pmatrix} \tilde{W}_L^- \\ \tilde{H}_{1L}^- \end{pmatrix}, \qquad \begin{pmatrix} \tilde{\chi}_{1R}^- \\ \tilde{\chi}_{2R}^- \end{pmatrix} = O_R \begin{pmatrix} \tilde{W}_R^- \\ \tilde{H}_{2R}^- \end{pmatrix}. \tag{2.29}$$

then the chargino mass eigenstates are given by

$$\tilde{\chi}_i^- = \tilde{\chi}_{iL}^- + \tilde{\chi}_{iR}^- \qquad (i = 1, 2) \tag{2.30}$$

One should note that if $M_2, \mu \approx \Lambda \gg M_W$, the diagonal elements dominate the chargino mass matrix and the diagonalizing matrix is close to the identity matrix. From Eq. 2.29, one could see that under such condition the left and right weyl components of a chargino is mostly a wino or a higgsino and there is relatively less mixing. Their masses can be approximated by M_2 and μ and corrections to this enters at $\sim \mathcal{O}(M_Z^2/\Lambda^2)$. This feature will be used later in our analysis.

From Eq. 2.30, we see how the four-component Dirac chargino can be written in terms of left chiral and right chiral weyl spinors.

Finally we come to neutralinos. The mass matrix of the neutralinos is given by

$$-\mathcal{L}_m = \frac{1}{2} \left(\tilde{B}_L \tilde{W}_L^0 \tilde{H}_{1L}^0 \tilde{H}_{2L}^0 \right) M_N \begin{pmatrix} \tilde{B}_L \\ \tilde{W}_L^0 \\ \tilde{H}_{1L}^0 \\ \tilde{H}_{2L}^0 \end{pmatrix} + h.c., \tag{2.31}$$

where

$$M_N = \begin{pmatrix} M_1 & 0 & -m_Z \sin\theta_W \cos\beta & m_Z \sin\theta_W \sin\beta \\ 0 & M_2 & m_Z \cos\theta_W \cos\beta & -m_Z \cos\theta_W \sin\beta \\ -m_Z \sin\theta_W \cos\beta & m_Z \cos\theta_W \cos\beta & 0 & -\mu \\ m_Z \sin\theta_W \sin\beta & -m_Z \cos\theta_W \sin\beta & -\mu & 0 \end{pmatrix}. \tag{2.32}$$

which is diagonalized by a real orthogonal matrix O_N,

$$O_N \mathcal{M}_\mathcal{N} O_N^\mathsf{T} = \mathcal{M}_\mathcal{N}^\mathcal{D} \tag{2.33}$$

The mass eigenstates are given by

$$\tilde{\chi}_{iL}^0 = (O_N)_{ij} \tilde{X}_{jL}^0 \qquad (i, j = 1, \cdots, 4) \tag{2.34}$$

14

where
$$\tilde{X}_{iL}^0 = (\tilde{B}_L, \tilde{W}_L^0, \tilde{H}_{1L}^0, \tilde{H}_{2L}^0).$$ (2.35)

We have thus Majorana spinors

$$\tilde{\chi}_i^0 = \tilde{\chi}_{iL}^0 + \tilde{\chi}_{iR}^0, \quad (i = 1, \cdots, 4)$$ (2.36)

with mass $M_{\tilde{\chi}_A^0}$.

$$\tilde{\chi}_i^0 = \tilde{\chi}_{iL}^0 + \tilde{\chi}_{iR}^0, \quad (i = 1, \cdots, 4)$$

Chapter 3

Constraints on Slepton Mass Matrix

As mentioned earlier, the lepton flavour is not conserved in general in supersymmetry owing to the off diagonal elements of the slepton mass matrix.This supersymmetric feature would contribute to the rare deacy of leptons via the following one loop diagrams
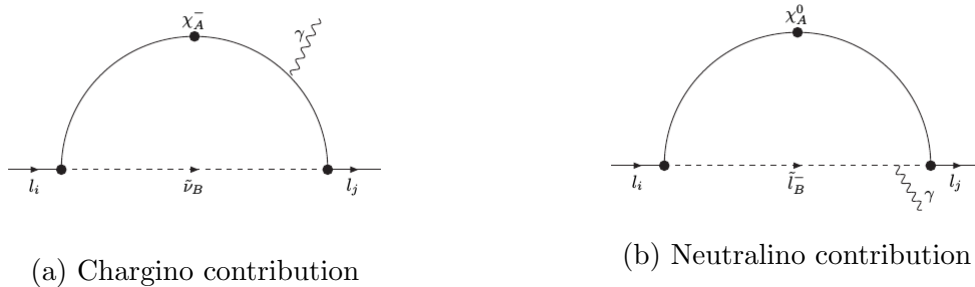

(a) Chargino contribution

(b) Neutralino contribution

Figure 3.1: One loop contribution to rare decay $l_i \to l_j \gamma$ a) via chargino, b) via neutralino in the internal leg

Since the $l_i \to l_j \gamma$ decay is highly suppressed in nature, any acceptable model of SUSY should comply with the constraints imposed by extremely stringent upper limits on rare decays put by experiments. Models like minimal Supergravity (mSUGRA), gauge mediated symmetry breaking (GMSB) and Anomaly mediated symmetry breaking(AMSB) may break SUSY in flavour blind fashion at high scales [6]. They predict a universal common value for slepton mass matrix which even after evolving to weak scale does not give rise to off-diagonal elements.

A problem of interest is to quantify the maximum amount of misalignment of slepton mass matrix allowed by the current data. To that end one uses the method of mass insertion to do the calculation. This involves calculating the effect of the off-diagonal entries in the mass matrix which is diagonal to begin with in the mass eigenstate basis of slepton. Consider once again the slepton mass matrix.

$$\mathcal{M}^2 = \begin{pmatrix} m_L^2 & m_{LR}^{2\mathsf{T}} \\ m_{LR}^2 & m_R^2 \end{pmatrix} \tag{3.1}$$

where m_L^2 and m_R^2 are 3×3 hermitian matrices and m_{LR}^2 is a 3×3 matrix. In the mass insertion approximation, these matrices are diagonal to begin with and a non-diagonal term $\Delta_{ij}^{AB} = \delta_{ij}^{AB} m_i^A m_j^B$ is inserted to introduce misalignment. Here the index i, j runs over the generation while $A, B = L, R$ refer to the left and right handed sleptons. To maintain the hermiticity of the matrix of the mass matrix, we assume $\Delta_{ij}^{AB} = \Delta_{ji}^{AB}$. For example, a mass insertion Δ_{12}^{LL} would appear in the m_L^2 matrix as

$$m_L^2 = \begin{pmatrix} m_{L11}^2 & \Delta_{12}^{LL} & 0 \\ \Delta_{12}^{LL} & m_{L22}^2 & 0 \\ 0 & 0 & m_{L33}^2 \end{pmatrix} \tag{3.2}$$

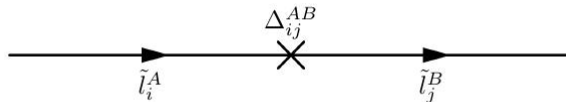which corresponds to a Feynman propagator shown in (3.2)

Figure 3.2: Feynman propagator depicting mass insertion

A compelete specification of the composition of neutralino and chargino would require specifics of a model. In order to keep the analysis model independent in the approximate calculation, the off-diagonal entries appearing in the neutralino and chargino mass matrices are assumed to be much smaller than the diagonal elements $M1, M2$ and μ. In other words, M_1, M_2 and $\mu \gg M_W$. Under this assumption, we have Feynman diagram like Fig. 3.3

Figure 3.3: Chirality flip in $\tilde{B}^0$ and $\tilde{W}^-$ for pure Bino and Wino eigenstates.

3.1 MIA Calculation

3.1.1 Amplitude for $l_i \to l_j \gamma$

The amplitude for the process $l_i \to l_j \gamma$ take the form

$$T = m_{l_i}\epsilon^\lambda \overline{u}_j(p-q)[iq^\nu \sigma_{\lambda\nu}(A_L P_L + A_R P_R)]u_i(p)$$

with q being the photon momentumin in the limit $q \to 0$. ϵ^λ is the photon polarization vector, while p is the momentum of the incoming lepton.The decay width is given by

$$\Gamma(l_i \to l_j\gamma) = \frac{48\pi^3\alpha}{G_f^2}(A_L^2 + A_R^2) \tag{3.3}$$

where G_f is the Fermi constant. In the mass insertion approximation, the left and right amplitudes are given by [15] [16]

$$
\begin{aligned}
(A_L^{ij}) &= \frac{\alpha_2}{4\pi}\Delta_{ij}^{LL}\left[\frac{f_{1n}(a_{L2}) + f_{1c}(a_{L2})}{m_{\tilde{L}}^4} + \frac{\mu M_2 tan\beta}{(M_2^2 - \mu^2)}\frac{(f_{2n}(a_{L2},b_L) + f_{2c}(a_{L2},b_L))}{m_{\tilde{L}}^4}\right] \\
&+ \frac{\alpha_1}{4\pi}\Delta_{ij}^{LL}\left[\frac{f_{1n}(a_L)}{m_{\tilde{L}}^4} + \mu M_1 tan\beta\left(\frac{-f_{2n}(a_L,b_L)}{m_{\tilde{L}}^4(M_1^2 - \mu^2)} + \frac{2f_{2n}(a_L)}{m_{\tilde{L}}^4(m_{\tilde{R}}^2 - m_{\tilde{L}}^2)}\right)\right] \\
&+ \frac{\alpha_1}{4\pi}\Delta_{ij}^{LL}\left[\frac{\mu M_1 tan\beta}{(m_{\tilde{R}}^2 - m_{\tilde{L}}^2)^2}\left(\frac{f_{3n}(a_R)}{m_{\tilde{R}}^2} - \frac{f_{3n}(a_L)}{m_{\tilde{L}}^2}\right)\right] \\
&+ \frac{\alpha_1}{4\pi}\Delta_{ij}^{LR}\left[\frac{1}{(m_{\tilde{L}}^2 - m_{\tilde{R}}^2)}\left(\frac{M_1}{m_{l_j}}\right)\left(\frac{f_{3n}(a_R)}{m_{\tilde{R}}^2} - \frac{f_{3n}(a_L)}{m_{\tilde{L}}^2}\right)\right]
\end{aligned} \tag{3.4}
$$

and

$$
\begin{aligned}
(A_R^{ij}) &= \frac{\alpha_1}{4\pi}\Delta_{ij}^{RR}\left[\frac{4f_{1n}(a_R)}{m_{\tilde{R}}^4} + \mu M_1 tan\beta\left(\frac{2f_{2n}(a_R,b_R)}{m_{\tilde{R}}^4(M_1^2 - \mu^2)} + \frac{2f_{2n}(a_R)}{m_{\tilde{R}}^4(m_{\tilde{L}}^2 - m_{\tilde{R}}^2)}\right)\right] \\
&+ \frac{\alpha_1}{4\pi}\Delta_{ij}^{RR}\left[\frac{\mu M_1 tan\beta}{(m_{\tilde{L}}^2 - m_{\tilde{R}}^2)^2}\left(\frac{f_{3n}(a_L)}{m_{\tilde{L}}^2} - \frac{f_{3n}(a_R)}{m_{\tilde{R}}^2}\right)\right] \\
&+ \frac{\alpha_1}{4\pi}\Delta_{ij}^{RL}\left[\frac{1}{(m_{\tilde{R}}^2 - m_{\tilde{L}}^2)}\left(\frac{M_1}{m_{l_j}}\right)\left(\frac{f_{3n}(a_L)}{m_{\tilde{L}}^2} - \frac{f_{3n}(a_R)}{m_{\tilde{R}}^2}\right)\right] ,
\end{aligned} \tag{3.5}
$$

where $\alpha_1 = (5/3)(\alpha/\cos^2\theta_W)$, $\alpha_2 = (\alpha/\sin^2\theta_W)$, $a_{L2} = M_2^2/m_{\tilde{L}}^2$, $a_L = M_1^2/m_{\tilde{L}}^2$, $a_R = M_1^2/m_{\tilde{R}}^2$, $b_L = \mu^2/m_{\tilde{L}}^2$, $b_R = \mu^2/m_{\tilde{R}}^2$, $\Delta_{ij}^{AB} = \delta_{ij}^{AB}m_{\tilde{A}}m_{\tilde{B}}$ and $m_{\tilde{L}}$ and $m_{\tilde{R}}$ are the average slepton masses for the left and right sleptons, respectively. The M_1 and M_2 are the gaugino mass parameters. The f_{in}'s and f_{ic}'s are loop functions from neutralinos and charginos contributions, respectively, given by:

$$
\begin{aligned}
f_{1n}(x) &= \frac{-17x^3 + 9x^2 + 9x - 1 + 6x^2(x+3)\ln x}{24(1-x)^5} , \\
f_{2n}(x) &= \frac{-5x^2 + 4x + 1 + 2x(x+2)\ln x}{4(1-x)^4} ,
\end{aligned}
$$

$$
\begin{aligned}
f_{3n}(x) &= \frac{1 + 2x \ln x - x^2}{2(1-x)^3} \,, \\
f_{1c}(x) &= \frac{-3 - 9x^2 + 9x + 1 + 6x(x+1)\ln x}{6(1-x)^5} \,, \\
f_{2c}(x) &= \frac{-x^2 - 4x + 5 + 2(2x+1)\ln x}{2(1-x)^4} \,, \\
f_{2n}(x,y) &= f_{2n}(x) - f_{2n}(y) \,, \\
f_{2c}(x,y) &= f_{2c}(x) - f_{2c}(y) \,.
\end{aligned}
\tag{3.6}
$$

3.1.2 Explanation of the terms and cancellation in amplitude

Of all the possible diagrams which contribute to the amplitude, two contributions are of great significance which result in cancellation in amplitude due to destructive interference. In the basis where the lepton masses and the gauge couplings are flavour diagonal, the lagrangian is given by [15]

$$
\begin{aligned}
-\mathcal{L} &= \tilde{l}_{Li}^{\dagger} \overline{\tilde{\chi}_A^0} \left(N_{LR}^{A(i)} P_R + N_{LL}^{A(i)} P_L \right) l_i + \tilde{l}_{Ri}^{\dagger} \overline{\tilde{\chi}_A^0} \left(N_{RR}^{A(i)} P_R + N_{RL}^{A(i)} P_L \right) l_i \\
&+ \tilde{\nu}_i^{\dagger} \overline{\tilde{\chi}_A^-} (C_{LR}^{A(i)} P_R + C_{LL}^{A(i)} P_L) l_i + h.c., \qquad i = e, \mu, \tau
\end{aligned}
\tag{3.7}
$$

where the coefficient $C_{B,C}^{A(i)}$ and $N_{B,C}^{A(i)}$ (with $B, C = (L, R)$) are:

$$
\begin{aligned}
C_{LL}^{A(i)} &= g_2 (O_R)_{A1} \\
C_{LR}^{A(i)} &= -\frac{g_1}{\sqrt{2}} \frac{m_{l_i}}{M_W c_\beta} (O_L)_{A2} \\
N_{LL}^{A(i)} &= -\frac{g_2}{\sqrt{2}} (O_N)_{A2} - \frac{g_1}{\sqrt{2}} (O_N)_{A1} \\
N_{RR}^{A(i)} &= \sqrt{2} g_1 (O_N)_{A1} \\
N_{LR}^{A(i)} &= N_{RL}^{A(i)} = \frac{g_1}{\sqrt{2}} \frac{m_{l_i}}{M_W c_\beta} (O_N)_{A3},
\end{aligned}
\tag{3.8}
$$

where $O_{L,R}$ and O_N diagonalize the chargino and neutralino mass matrices, respectively.

Consider figure 3.4a having a $\widetilde{B}^0$ exchange with a flavor violating and a chirality flipping term in the internal slepton line. In this case, both the incoming and outgoing chiral leptons couple with a slepton of same chirality at the vertices. As a result the amplitude is proportional to N_{RR} and N_{LL}. The terms N_{RR} and N_{LL} have opposite sign with respect to each other as can be seen in Eq. (3.8). In addition, the amplitude is proportional to the M_1 ($\widetilde{B}^0$ mass), $\mu \tan\beta$ (the L-R mass slepton mass term) apart from the mass insertion term Δ_{ij}^{AB}. Since its proportional to $\tan\beta$ the contribution is enhanced with increase in the magnitude of β. On the other hand, a $\widetilde{B}^0$-$\widetilde{H}^0$ exchange (3.4b) with chirality flipped at one of the vertex through yukawa term, has a left lepton coupling to a right slepton and higgsino at one vertex while a right slepton-right lepton-bino coupling

at another. The term thus is proportonal to N_{RL} and N_{RR} which have the same sign (3.25). Moreover this contribution too is tanβ enhanced, where the tanβ comes from the presence of yukawa coupling ($\propto 1/\cos(\beta)$) and $\widetilde{B}^0$-$\widetilde{H}^0$ mixing which is proportion to $\sin(\beta)$. In addition the numerator has M_1 ($\widetilde{B}^0$ mass), μ ($\widetilde{H}^0$ mass) and of course Δ_{ij}^{AB}. As we can see we have two contributions of same order coming with opposite signs. This results in the cancellation in the amplitude contributing to $\text{Br}(l_j \to l_i)$ and the constraints are expected to be relaxed in certain regions of parameter space. These cancellations were shown by Hisano et al [17]
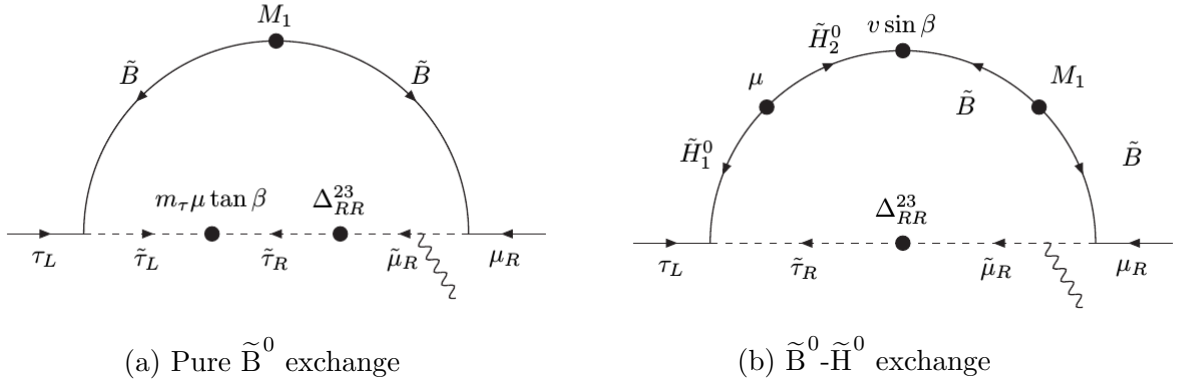

(a) Pure $\widetilde{B}^0$ exchange (b) $\widetilde{B}^0$-$\widetilde{H}^0$ exchange

Figure 3.4: Diagrams contributing to cancellation of amplitude[17].

3.1.3 Parameterization and Results

Under MIA, we wrote a Python program to plot the $\text{Br}(l_i \to l_j\gamma)$ versus δ for 1-2 and 2-3 generation for 3 model points PS1, PS2, PS3 which are defined as follows

$$PS1: \ M_1 = 300, \ M_2 = 600, \ m_L = 500, \ m_R = 450, \ \mu = 350, \ tan\beta = 20$$
$$PS2: \ M_1 = 250, \ M_2 = 500, \ m_L = 475, \ m_R = 525, \ \mu = 375, \ tan\beta = 20$$
$$PS3: \ M_1 = 250, \ M_2 = 500, \ m_L = 625, \ m_R = 650, \ \mu = 600, \ tan\beta = 20$$

Figure 3.5: Branching fraction versus δ for parameter set PS1. The black line corresponds to the 90% branching fraction limit coming from the rare decay experiments 1.1
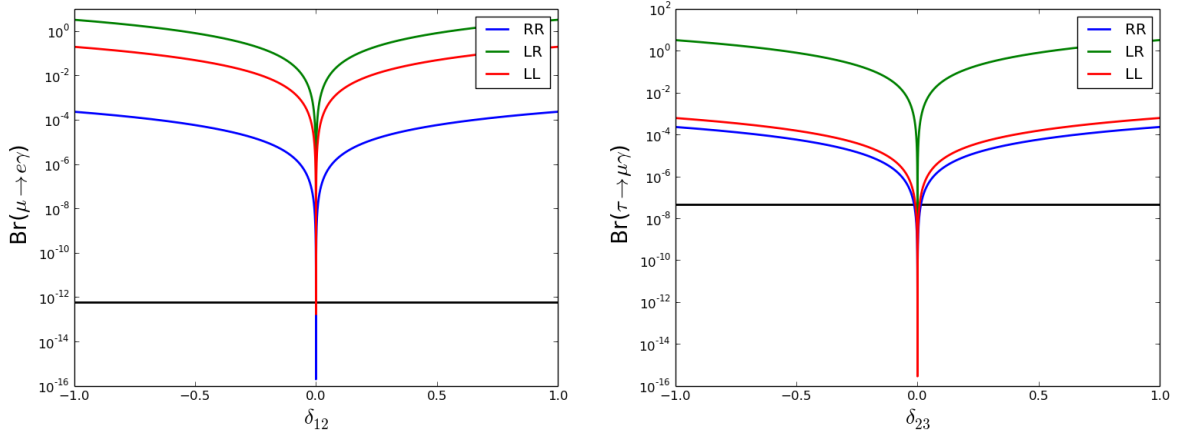

Figure 3.6: Branching fraction versus δ for parameter set PS2. The black line corresponds to the 90% branching fraction limit coming from the rare decay experiments 1.1

Figure 3.7: Branching fraction versus δ for parameter set PS3. The black line corresponds to the 90% branching fraction limit coming from the rare decay experiments 1.1
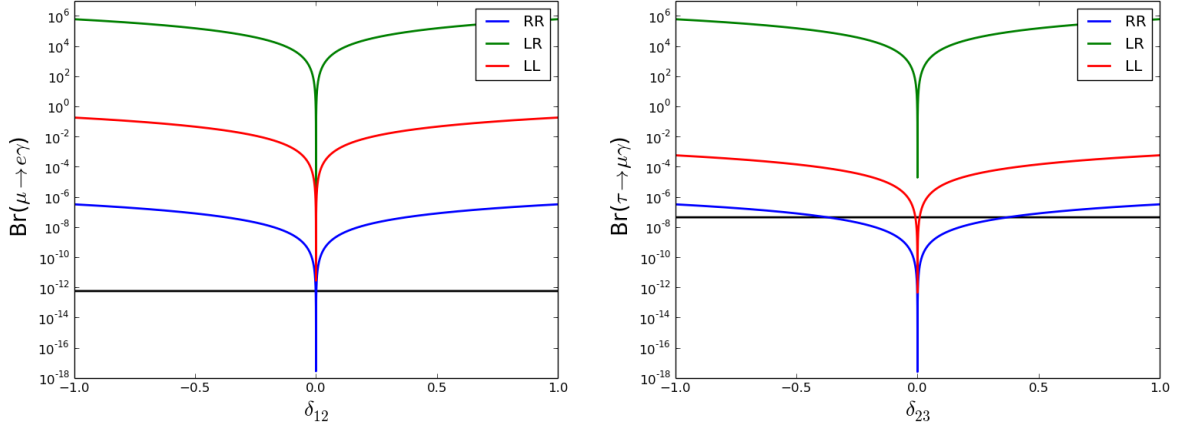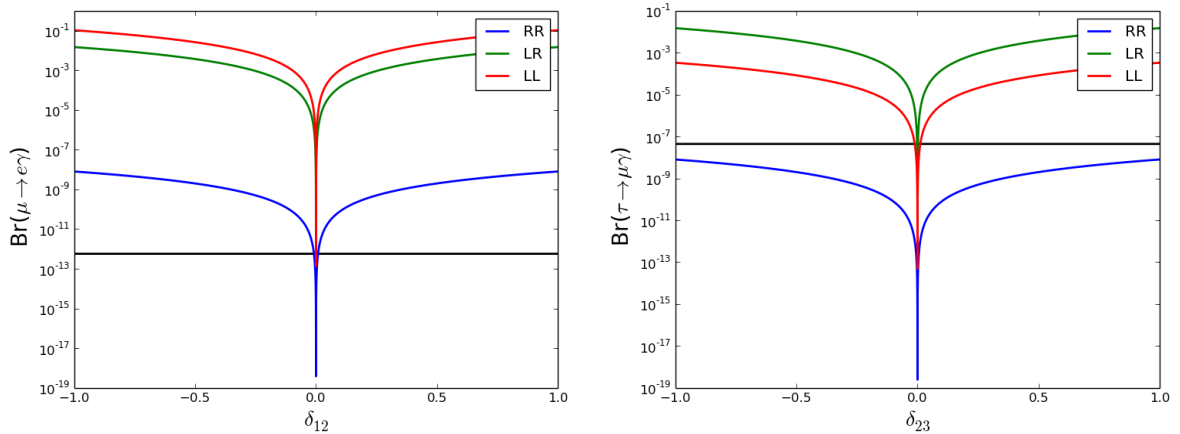
In the above calculation, we use the parameter sets defined on the pervious page and randomly vary δ over a range (-1.0,1.0) to get the branching fraction using Eq. 3.3 - 3.5. From the figure we see that, as —δ— increases in magnitude, the branching fraction for the rare decay increases uniformly. In 1-2 generation, where the bound on rare decay $\mu \to e\gamma$ is of $\mathcal{O}(10^{-13})$, the branching ratios for non-negligible values of δ are usually above the experimental bound indicated by the black line in the figure. For 2-3 generation, the bounds are not that strong ($\mathcal{O}(10^{-8})$) and therefore even a relatively larger δ of $\mathcal{O}(10^{-1})$ gives branching fraction which are not excluded by experiments. Moreover, we can see that the cancellation in the RR sector is quite apparent. For all the three parameter sets (PS1, PS2 and PS3), the branching fraction for a given value of δ is least for the RR sector. Further the stronger bounds in 1-2 generation means that even with cancellation in the RR sector, the δ's permissable by rare decay constraints are vanishingly small. Only in the 2-3 sector, where the rare decay bounds are not so strong, we can have a significant value of δ within the rare decay limit for certain region of parameter space. In the above diagram, maximum allowed value of δ_{23} increases from PS1 ($\mathcal{O}(10^{-2})$) to PS2 ($\mathcal{O}(10^{-1})$) and from PS2 to PS3 ($\mathcal{O}(1)$).

These initial results seemed positive and therefore we moved on to doing full calculation under mass-insertion. For this the model needed to be specified beforehand. We worked in phenomenological minimal supersymmetric model (pMSSM) with flavour violation incorporated through mass insertion Δ_{ij}^{AB}

3.2   Full Calculation:

The mass insertion approximation is accurate only in the limit of small δ and small mass splittings of mass eigenvalue. [15]. Therefore we also perform the full calculation. The mass insertion of Δ_{ij}^{AB} in the diagonal slepton mass matrix makes it non-diagonal. As a result we need a non-trivial unitary matrix to dioganlize the mass matrix. This unitary matrix which was digonal for the approximate calculation is no more digonal and has non-trivial entries which can couple slepton and lepton of two different flavours at a slepton-lepton-neutralino vertex. Also as a result of the mass insertion Δ_{ij}^{AB}, the mass eigenvalues of the slepton $\tilde{l}_{iR}$ and and $\tilde{l}_{jR}$ become corelated through the insertion. The mass matrix looks like

$$
\mathcal{M}^2 = \begin{pmatrix}
m_{\tilde{e}_L}^2 & 0 & 0 & m_{LR}^e & 0 & 0 \\
0 & m_{\tilde{\mu}_L}^2 & 0 & 0 & m_{LR}^\mu & 0 \\
0 & 0 & m_{\tilde{\tau}_L}^2 & 0 & 0 & m_{LR}^\tau \\
m_{LR}^e & 0 & 0 & m_{\tilde{e}_R}^2 & 0 & 0 \\
0 & m_{LR}^\mu & 0 & 0 & m_{\tilde{\mu}_R}^2 & \Delta_{23}^{RR} \\
0 & 0 & m_{LR}^\tau & 0 & \Delta_{23}^{RR} & m_{\tau_R^2}^2
\end{pmatrix} \tag{3.9}
$$

where $m_{LR}^i = A_i - m_{l_i}\mu\tan\beta$ and $i = e,\mu,\tau$

On solving the following matrix equation

$$U\mathcal{M}^2 U^T = \mathcal{M}_D^2 \tag{3.10}$$

we get diagonalizing matrix U which is used for full calculation.

3.2.1 Amplitude for $l_i \to l_j\gamma$:

The neutralino contributions are given by [14] [18]

$$
\begin{aligned}
A^{(n)L} &= \frac{1}{32\pi^2}\frac{1}{m_{\tilde{l}_X}^2}\left[N_{iAX}^L N_{jAX}^{L*}\frac{1 - 6x_{AX} + 3x_{AX}^2 + 2x_{AX}^3 - 6x_{AX}^2\log x_{AX}}{6\left(1 - x_{AX}\right)^4}\right.\\
&\quad+ N_{iAX}^R N_{jAX}^{R*}\frac{m_j}{m_i}\frac{1 - 6x_{AX} + 3x_{AX}^2 + 2x_{AX}^3 - 6x_{AX}^2\log x_{AX}}{6\left(1 - x_{AX}\right)^4}\\
&\quad\left.+ N_{iAX}^L N_{jAX}^{R*}\frac{m_{\tilde{\chi}_A^0}}{m_i}\frac{1 - x_{AX}^2 + 2x_{AX}\log x_{AX}}{\left(1 - x_{AX}\right)^3}\right], \tag{3.11}\\
A^{(n)R} &= \left.A^{(n)L}\right|_{L\leftrightarrow R}, \tag{3.12}
\end{aligned}
$$

where $x_{AX} = m_{\tilde{\chi}_A^0}^2/m_{\tilde{l}_X}^2$ and the indices are $A = 1,..,4$, $X = 1,..,6$.

The chargino contributions are given by

$$
\begin{aligned}
A^{(c)L} &= -\frac{1}{32\pi^2}\frac{1}{m_{\tilde{\nu}_X}^2}\left[C_{iAX}^L C_{jAX}^{L*}\frac{2 + 3x_{AX} - 6x_{AX}^2 + x_{AX}^3 + 6x_{AX}\log x_{AX}}{6\left(1 - x_{AX}\right)^4}\right.\\
&\quad+ C_{iAX}^R C_{jAX}^{R*}\frac{m_j}{m_i}\frac{2 + 3x_{AX} - 6x_{AX}^2 + x_{AX}^3 + 6x_{AX}\log x_{AX}}{6\left(1 - x_{AX}\right)^4}\\
&\quad\left.+ C_{iAX}^L C_{jAX}^{R*}\frac{m_{\tilde{\chi}_A^-}}{m_i}\frac{-3 + 4x_{AX} - x_{AX}^2 - 2\log x_{AX}}{\left(1 - x_{AX}\right)^3}\right], \tag{3.13}\\
A^{(c)R} &= \left.A^{(c)L}\right|_{L\leftrightarrow R}, \tag{3.14}
\end{aligned}
$$

where in this case $x_{AX} = m_{\tilde{\chi}_A^-}^2/m_{\tilde{\nu}_X}^2$ and the indices are $A = 1,2$, $X = 1,2,3$. Notice that in both neutralino and chargino contributions a summation over the indices A and X is understood.

where the coefficients are

$$
\begin{aligned}
C_{iAX}^{R(l)} &= C_{LL}^{A(i)}U_{X,i}^\nu,\\
C_{iAX}^{L(l)} &= C_{LR}^{A(i)}U_{X,i}^\nu,\\
N_{iAX}^{R(l)} &= N_{LL}^{A(i)}U_{X,i}^l + N_{LR}^{A(i)}U_{X,i+3}^l,\\
N_{iAX}^{L(l)} &= N_{RL}^{A(i)}U_{x,i}^l + N_{RR}^{A(i)}U_{X,i+3}^l
\end{aligned} \tag{3.15}
$$

where the coefficient $C_{B,C}^{A(i)}$ and $N_{B,C}^{A(i)}$ are defined in 3.8.

3.2.2 Parameterization and Results:

MSSM in general has 105 supersymmetric and 19 standard model parameters. However experiments have put constraints on the parameter space especially on the CP violating phases. The CP violating phases result in large elctric dipole moments contradicting the experimental results [19]. While it is possible to find regions of parameter space where cancellations among different amplitudes allow large CP violating phases, inspite of the stringent EDM constraints [20], since such a region is by necessity somewhat restricted, we have decided to work in the situation where CPV phases are absent .Hence in our analysis we assume no CP violating phases and take our parameters to be real which reduces the number of independent parameters significantly. We take into account the exlusion limits set by LEP and LHC [21]on the sparticle masses and also the discovery potential of the next LHC run. With these in mind we wrote a Python program to perform a random scan over the parameter range: where δ is related to off-diagonal element Δ as

$$\Delta_{AB}^{ij} = \delta_{AB}^{ij} m_A^i m_B^j \tag{3.16}$$

with $A, B = L, R$ and i, j are generation indices.

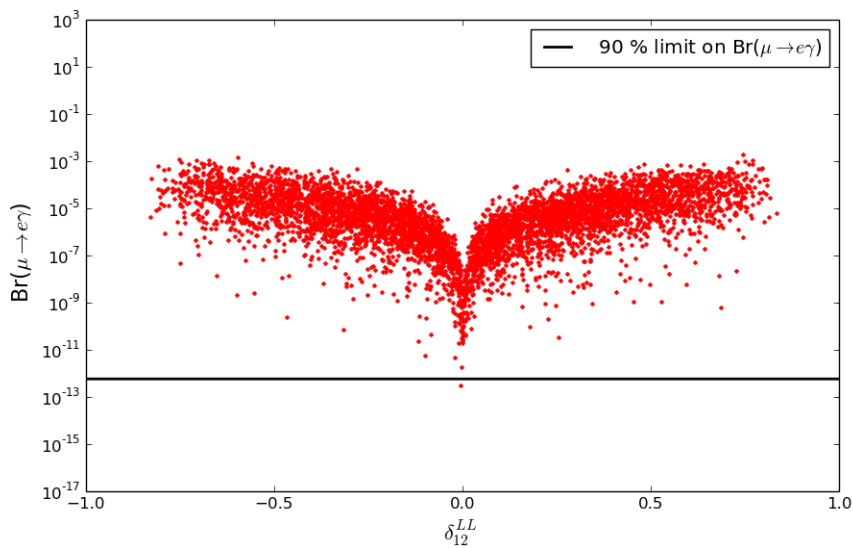| pMSSM parameters			
$m_{\tilde{e}_L}$	200 - 500	$m_{\tilde{\mu}_L}$	200 - 500
$m_{\tilde{\tau}_L}$	200 - 500	$m_{\tilde{e}_R}$	200 - 500
$m_{\tilde{\mu}_R}$	200 - 500	$m_{\tilde{\tau}_R}$	200 - 500
A_τ	400	M_1	40-600
M_2	103-600	μ	100-1000
$\tan\beta$	10-30	δ	-1.0 - 1.0

Figure 3.8: Scatter plot for BR$(\mu \to e\gamma)$ vs δ_{12}^{LL}. The horizontal black line indicates the experimental upper bound at 90% confidence level as quoted in 1.1. The points falling above the black line are exluded by experiments.

Figure 3.9: Scatter plot for BR($\mu \to e\gamma$) vs δ_{12}^{LR}. The horizontal black line indicates the experimental upper bound at 90% confidence level as quoted in 1.1. The points falling above the black line are exluded by experiments.
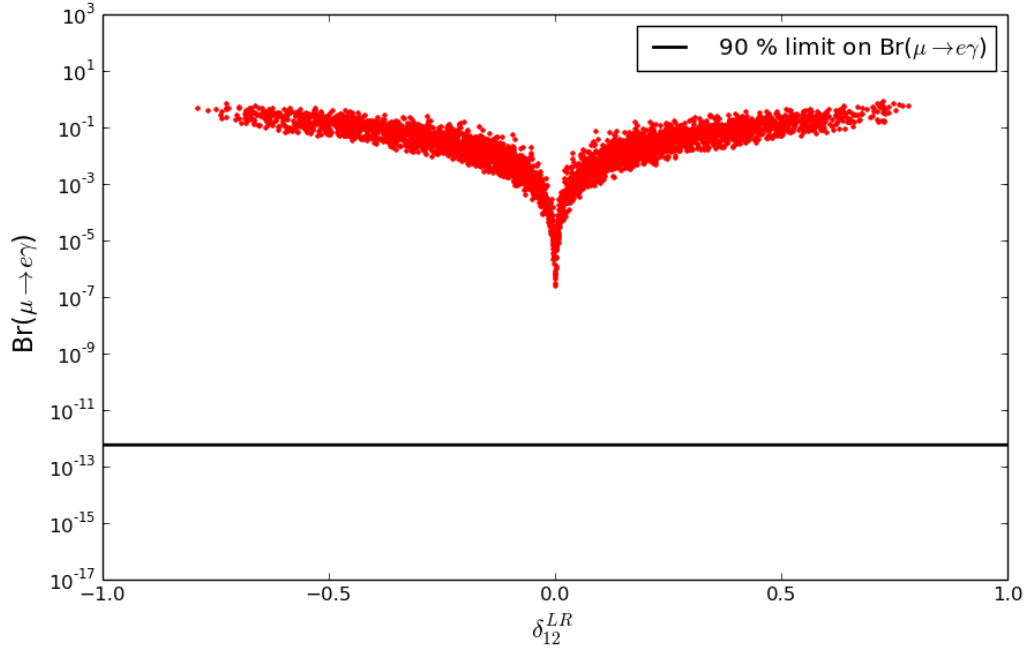

Figure 3.10: Scatter plot for BR($\mu \to e\gamma$) vs δ_{12}^{RR}. The horizontal black line indicates the experimental upper bound at 90% confidence level as quoted in 1.1. The points falling above the black line are exluded by experiments.

Figure 3.11: Scatter plot for $\mathrm{BR}(\tau \to e\gamma)$ vs δ_{13}^{LL}. The horizontal black line indicates the experimental upper bound at 90% confidence level as quoted in 1.1. The points falling above the black line are exluded by experiments.
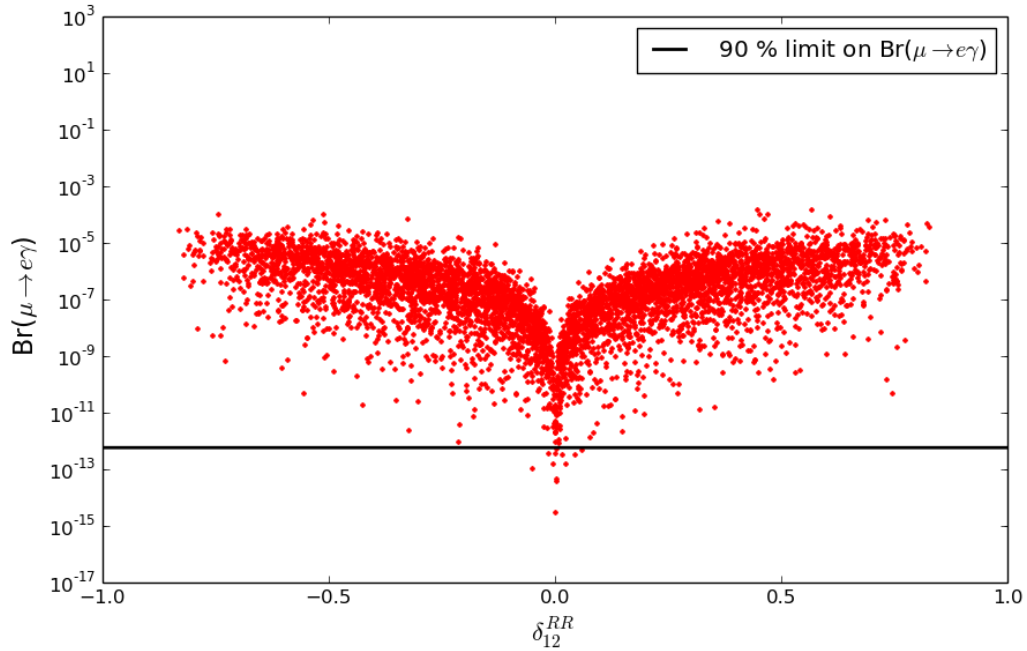

Figure 3.12: Scatter plot for $\mathrm{BR}(\tau \to e\gamma)$ vs δ_{13}^{LR}. The horizontal black line indicates the experimental upper bound at 90% confidence level as quoted in 1.1. The points falling above the black line are exluded by experiments.
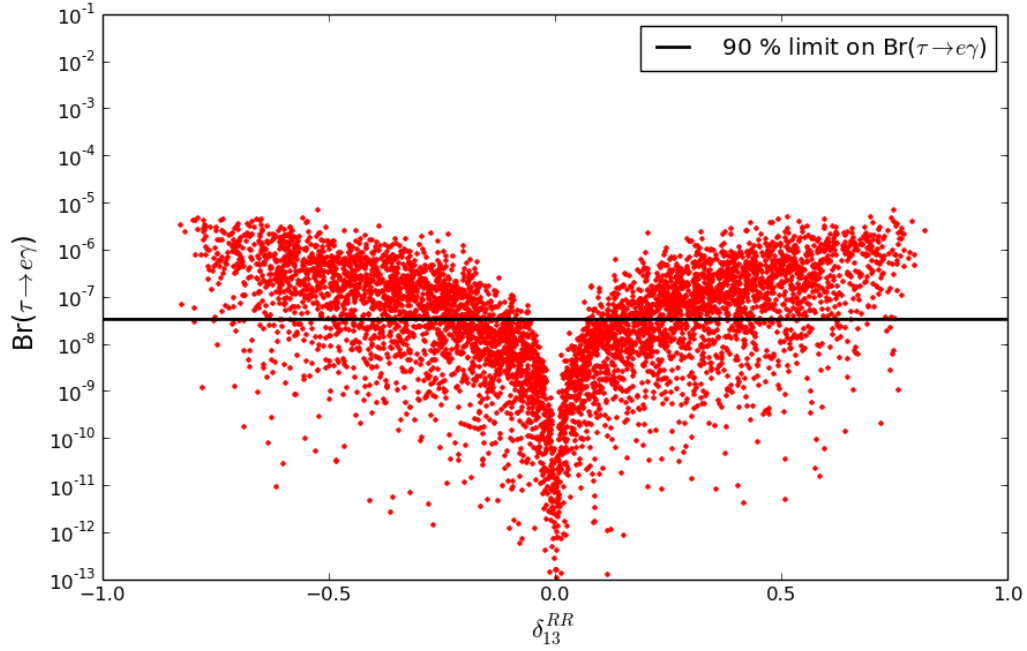
Figure 3.13: Scatter plot for BR($\tau \to e\gamma$) vs δ_{13}^{RR}. The horizontal black line indicates the experimental upper bound at 90% confidence level as quoted in 1.1. The points falling above the black line are exluded by experiments.
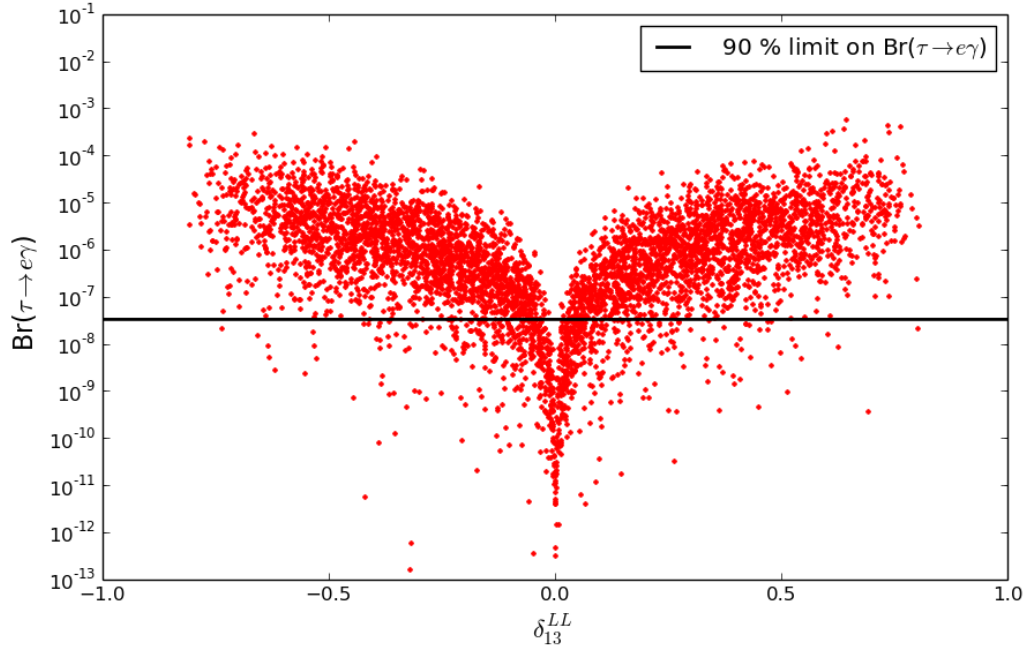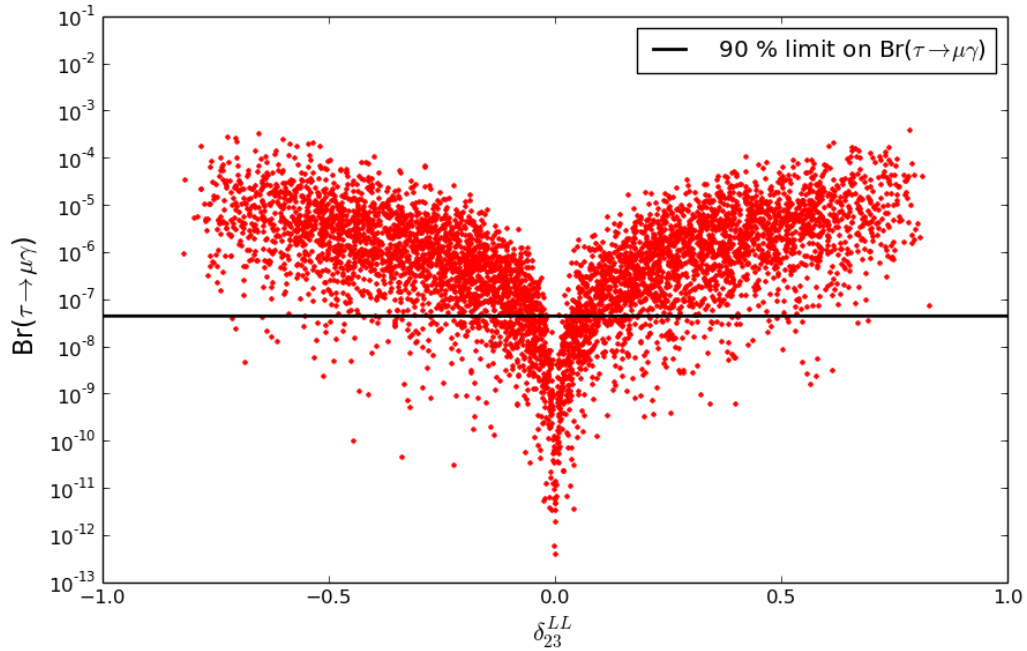

Figure 3.14: Scatter plot for BR($\tau \to \mu\gamma$) vs δ_{23}^{LL}. The horizontal black line indicates the experimental upper bound at 90% confidence level as quoted in 1.1. The points falling above the black line are exluded by experiments.
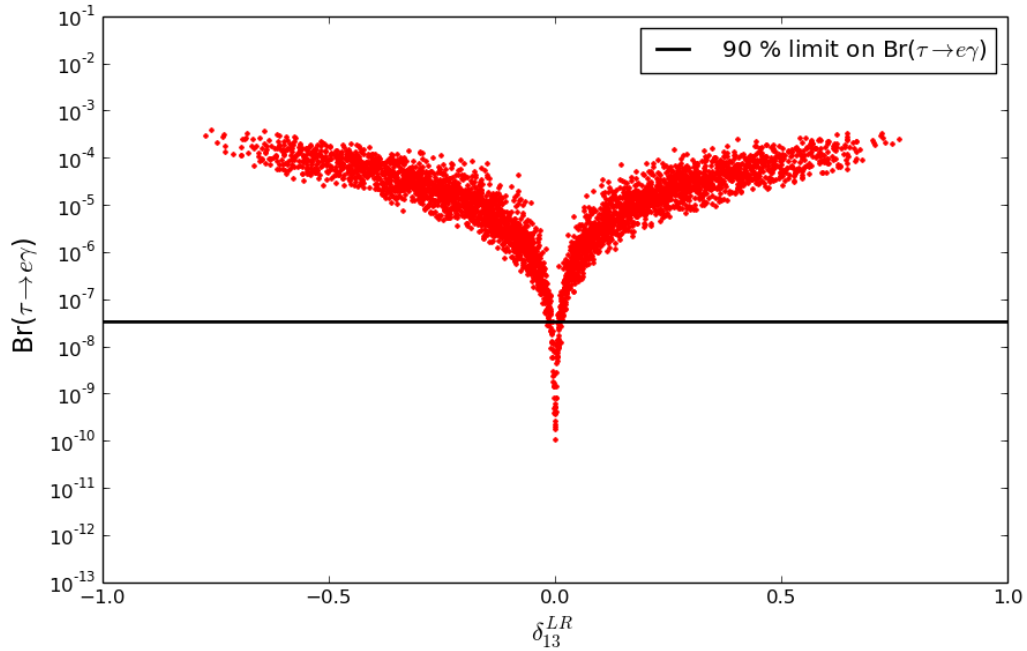
Figure 3.15: Scatter plot for BR($\tau \to \mu\gamma$) vs δ_{23}^{LR}. The horizontal black line indicates the experimental upper bound at 90% confidence level as quoted in 1.1. The points falling above the black line are exluded by experiments.

Figure 3.16: Scatter plot for BR($\tau \to \mu\gamma$) vs δ_{23}^{RR}. The horizontal black line indicates the experimental upper bound at 90% confidence level as quoted in Table1.1. The points falling above the black line are exluded by experiments.
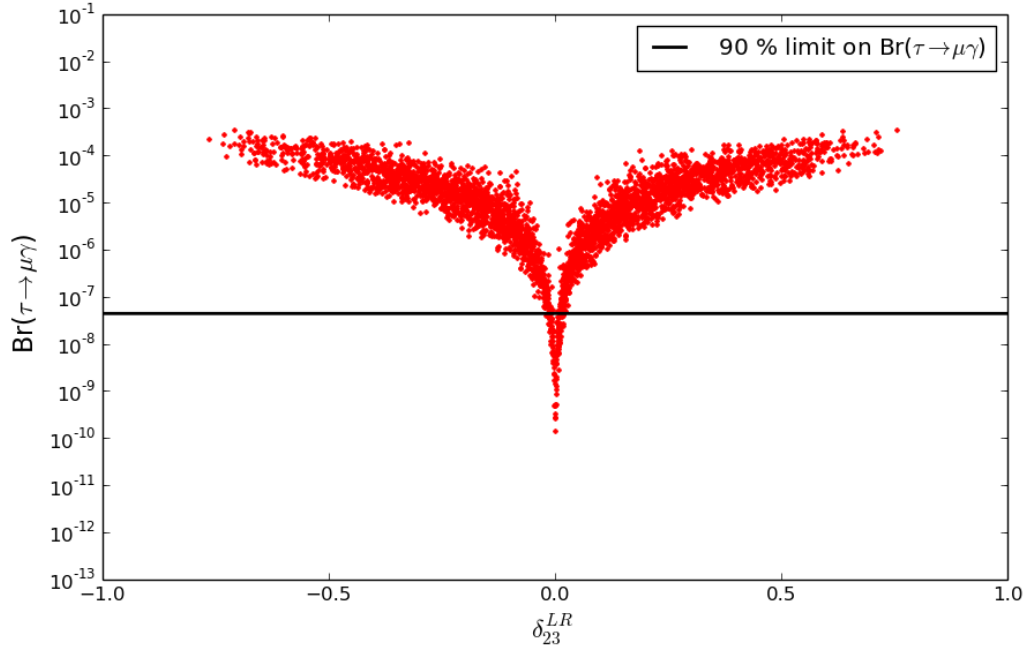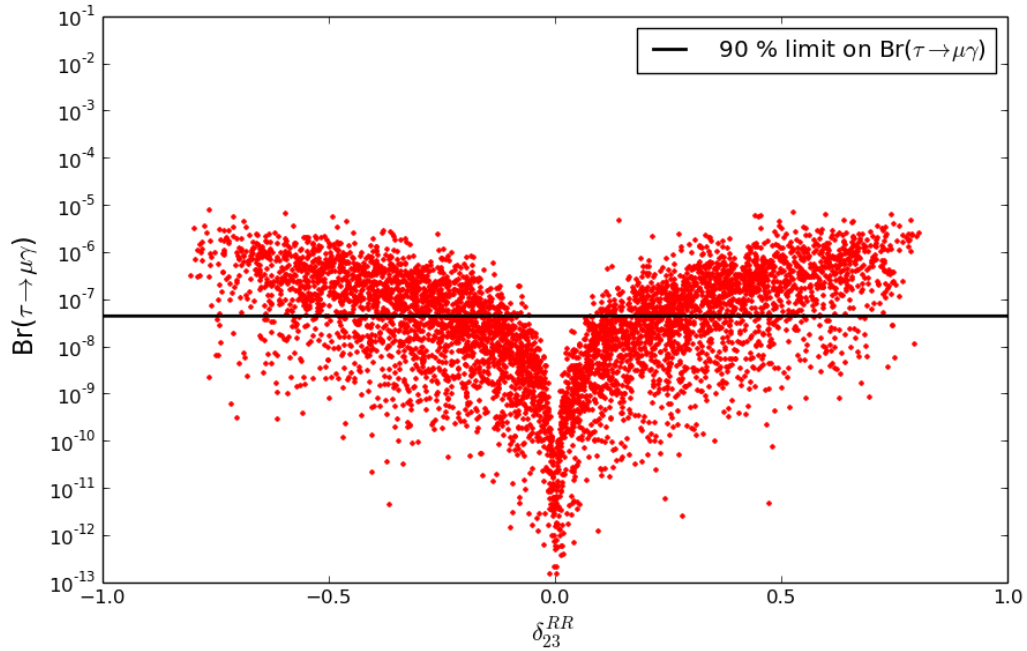
From the above figures, we observe that the constraints on 1-2 generation are very

strong as for a significant value of δ (where $\delta_{ij} = \Delta m_i m_j$), the braching ratio for rare decay is usually more than the 90% CL upper bound as indicated by the black line in the figure. However for 1-3 and 2-3 generations, substantially large values of mass insertion parameters are allowed even with the rather stringent upper limits on rare decays and values of δ upto 0.7-0.8 are possible. As far as chiral sectors are concerned, the mass insertion in L-R sector is much more constrained than in the LL or the RR sector . Although values of mass insertion parameter δ as large as 0.8 are allowed for both the RR and the LL sector for the 1-2 and 2-3 generation case, the trend in the RR sector is more pronounced than in the LL sector. The most robust least upper bound on δ which is valid throughout the parameter space studied, irrespective of any cancellation, are shown in the table below.

Bounds on δ	
δ_{12}^{LL}	1×10^{-5}
δ_{12}^{LR}	1.8×10^{-7}
δ_{12}^{RR}	4×10^{-5}
δ_{13}^{LL}	0.008
δ_{13}^{LR}	0.0025
δ_{13}^{RR}	0.03
δ_{23}^{LL}	0.008
δ_{23}^{LR}	0.0025
δ_{23}^{RR}	0.04

Table 3.1: Least upper bounds on δ from rare decay of leptons for the parameter space considered in our analysis.

3.3 The Inverse problem: A model independent approach

Consider the scenario where we know the slepton mass eigenvalues. We are interested in solving the inverse problem for the left sector of 1-2 generation as it would be a model independent procedure.

The slepton mass matrix with off-digonal element in the LL sector of 1-2 generation looks like

$$
\mathcal{M}^2 = \begin{pmatrix}
m_{\tilde{e}_L}^2 & \Delta_{12}^{LL} & 0 & m_{LR}^e & 0 & 0 \\
\Delta_{12}^{LL} & m_{\tilde{\mu}_L}^2 & 0 & 0 & m_{LR}^\mu & 0 \\
0 & 0 & m_{\tilde{\tau}_L}^2 & 0 & 0 & m_{LR}^\tau \\
m_{LR}^e & 0 & 0 & m_{\tilde{e}_R}^2 & 0 & 0 \\
0 & m_{LR}^\mu & 0 & 0 & m_{\tilde{\mu}_R}^2 & 0 \\
0 & 0 & m_{LR}^\tau & 0 & 0 & m_{\tilde{\tau}_R^2}
\end{pmatrix} \tag{3.17}
$$

Since the L-R mixing in first and second generation is suppressed by small lepton mass, we take a simplified picture with LR mixing in these generations set to 0. Since there is

only one flavour violating term in the slepton mass matrix which couples the left sector of first generation with the second generation, the third generation is decoupled from from 1-2 generation. Notice that the LR term for third generation is a flavour conserving term and mixes the stops together without affecting the selectron and smuons. Since the LR term for the first and second generation is set to 0, the LL sector of 1-2 generation is decoupled from the RR sector. In the diagonalizing matriz, we will have non-trivial flavour violating off-diagonal elements in the firt row second column and second row first column only. The other non-trivial off-diagonal element in would only mix the left-right stops together and would not couple the third generation with remaining generations. Thus our problem reduces to solving for top left 2×2 The reduced 2×2 satisfy the relation

$$\begin{pmatrix} \cos\theta & -\sin\theta \\ \sin\theta & \cos\theta \end{pmatrix} \begin{pmatrix} M_1^2 & \Delta_{LL}^{12} \\ \Delta_{LL}^{12} & M_2^2 \end{pmatrix} \begin{pmatrix} \cos\theta & \sin\theta \\ -\sin\theta & \cos\theta \end{pmatrix} = \begin{pmatrix} m^2 & 0 \\ 0 & m^2 + \Delta m^2 \end{pmatrix}$$

or

$$\begin{pmatrix} M_1^2 & \Delta_{LL}^{12} \\ \Delta_{LL}^{12} & M_2^2 \end{pmatrix} = \begin{pmatrix} \cos\theta & \sin\theta \\ -\sin\theta & \cos\theta \end{pmatrix} \begin{pmatrix} m^2 & 0 \\ 0 & m^2 + \Delta m^2 \end{pmatrix} \begin{pmatrix} \cos\theta & -\sin\theta \\ \sin\theta & \cos\theta \end{pmatrix}$$

which gives us

$$\begin{pmatrix} M_1^2 & \Delta_{LL}^{12} \\ \Delta_{LL}^{12} & M_2^2 \end{pmatrix} = \begin{pmatrix} m^2 + \Delta m^2 \sin^2\theta & \Delta m^2 \sin\theta \cos\theta \\ \Delta m^2 \sin\theta \cos\theta & m^2 + \Delta m^2 \cos^2\theta \end{pmatrix}$$

One should note that in the limit $\Delta m^2 \to 0$, the off-diagonal terms vanish and the diagonal terms become equal to the degenerate common mass m^2. This means that $\mathrm{BR}(l_j \to l_i \gamma)$ also vanishes.

Expanding and equating the off-diagonal term,

$$\Delta_{LL}^{12} = \delta M_1 M_2 = \Delta m^2 \sin\theta \cos\theta \tag{3.21}$$

substituting for M_1 and M_2 in the above equation, we get

$$\delta_{LL}^{12} \sqrt{m^2 + \Delta m^2 \sin^2\theta} \sqrt{m^2 + \Delta m^2 \cos^2\theta} = \Delta m^2 \sin\theta \cos\theta \tag{3.22}$$

$$\delta_{LL}^{12} m^2 \sqrt{\left(1 + \frac{\Delta m^2}{m^2} \sin^2 \theta\right) \left(1 + \frac{\Delta m^2}{m^2} \cos^2 \theta\right)} = \Delta m^2 \sin \theta \cos \theta \tag{3.23}$$

$$\delta_{LL}^{12} m^2 \sqrt{1 + \frac{\Delta m^2}{m^2} + \left(\frac{\Delta m^2}{m^2}\right)^2 \sin^2 \theta \cos^2 \theta} = \Delta m^2 \sin \theta \cos \theta \tag{3.24}$$

Taking term of $\mathcal{O}(1)$, we have the simple equation

$$\delta_{LL}^{12} = \frac{\Delta m^2 \sin \theta \cos \theta}{m^2} \tag{3.25}$$

Thus the constraint on delta indirectly constrains the product $\frac{\Delta m^2 \sin \theta \cos \theta}{m^2}$. If δ_{max} is the maximum insertion allowed then the condition

$$\frac{|\Delta m^2 \sin \theta \cos \theta|}{m^2} < \delta_{max} \tag{3.26}$$

must hold. Similar results were obtained in [22] using a different approach. Now, $|\sin \theta \cos \theta|$ belongs to $[0, \frac{1}{2}]$. Therefore, θ is unconstrained if

$$\frac{1}{2} < \frac{\delta_{max} m^2}{\Delta m^2} \tag{3.27}$$

3.4   LFV branching ratio for neutralino

From the above formalism, the slepton eigenstates in mass eigenstate basis of lepton and neutralino can be written as

$$\begin{pmatrix} \tilde{e}_L \\ \tilde{\mu}_L \end{pmatrix} = \begin{pmatrix} \cos \theta & \sin \theta \\ -\sin \theta & \cos \theta \end{pmatrix} \begin{pmatrix} \tilde{e}_{L_m} \\ \tilde{\mu}_{L_m} \end{pmatrix}$$

Where $\tilde{e}_L$ and $\tilde{\mu}_L$ are now mixture of the mass eigenstates e_{L_m} and μ_{L_m}. The e_{L_m} component in e_L is changed by a factor $\cos \theta$ while the μ_L now gets a component of ϵ_{L_m} proportional to $\sin \theta$. Similar mixing happens in case of μ_{Lm}. As a result of this, we get flavour violating decays of sleptons. The branching ratios are modified in the following ways

$$Br_v(\chi_2^0 \to \tilde{e}e) = \cos^2 \theta Br_{nv}(\chi_2^0 \to \tilde{e}e)$$

$$Br_v(\chi_2^0 \to \tilde{\mu}\mu) = \cos^2 \theta Br_{nv}(\chi_2^0 \to \tilde{\mu}\mu) \tag{3.29}$$

$$Br_v(\chi_2^0 \to \tilde{\mu}e) = \sin^2 \theta Br_{nv}(\chi_2^0 \to \tilde{e}e)$$

$$Br_v(\chi_2^0 \to \tilde{e}\mu) = \sin^2 \theta Br_{nv}(\chi_2^0 \to \tilde{\mu}\mu) \tag{3.30}$$

where Br_v is the branching ratio in case of flavour violation while Br_{nv} is the branching ratio in case of no flavour violation The sleptons then decay to a lepton and the lightest neutralino through another lepton-slepton-neutralino vertex where the same analysis holds. A flavour violating $e\mu\widetilde{\chi}_1^0$ results if there is LFV at one of the two vertex with flavour conservation at the other. The flavour violating branching fraction is given by

$$Br(\tilde{\chi}_2^0 \to e\mu\widetilde{\chi}_1^0) = \sin^2\theta\cos^2\theta Br(\tilde{\chi}_2^0 \to ee\widetilde{\chi}_1^0) + \sin^2\theta\cos^2\theta Br(\tilde{\chi}_2^0 \to \mu\mu\widetilde{\chi}_1^0) \quad (3.31)$$

where $Br(\tilde{\chi}_2^0 \to ee\widetilde{\chi}_1^0)$ and $Br(\tilde{\chi}_2^0 \to \mu\mu\widetilde{\chi}_1^0)$ is the branching ratio of $\tilde{\chi}_2^0$ in the case where there is no mixing at the interaction vertex.

Chapter 4

Signals of SLFV

Lepton flavour violation can be exhibited in the following direct decay channels

$$\widetilde{\ell}_j \to \ell_k \widetilde{\chi}^0_i$$

$$\widetilde{\ell}_j \to \nu_k \widetilde{\chi}^\pm_i$$

$$\widetilde{\nu}_j \to \ell_k \widetilde{\chi}^\pm_i$$

$$\widetilde{\nu}_j \to \nu_k \widetilde{\chi}^0_i$$

However, since the neutrinos leave the detector undetected, the decay into a neutrino is not an experimentally useful process to observe LFV. This leaves us with the slepton/sneutrino decay into charged lepton for investigating LFV.

$$pp \to \overline{\widetilde{\ell}}_i \widetilde{\ell}_i \to \ell_k \ell_j \widetilde{\chi}^0_1 \widetilde{\chi}^0_1$$

The Drell-Yan process can give a pair of sleptons/sneutrinos of same flavour which can decay to two opposite sign leptons of different flavour [22] . The background to the process comes from $\bar{t}$ t, W^+ W^- production and decay and it is usually difficult to extract the signal from the background. A relatively low cross-section for the SUSY Drell-Yan does not help either.

$$\widetilde{\chi}^0_2 \to \ell_i \widetilde{\ell}_j \to \ell_i \ell_k \widetilde{\chi}^0_1$$

A highly studied channel for lepton flavour violation is the decay of neutralino (mostly $\widetilde{\chi}^0_2$) to a lepton and a slepton with subsequent decay of the slepton to a lepton of different flavour along with $\widetilde{\chi}^0_1$. The channel is kinematically open only if $\widetilde{\chi}^0_2$ is heavier than slepton [23, 24].

$\widetilde{\chi}^0_2$ can also be produced in the decay of gluino and squarks [22]. Since the gluino/squarks are produced via strong interaction, their production cross-section can be significantly
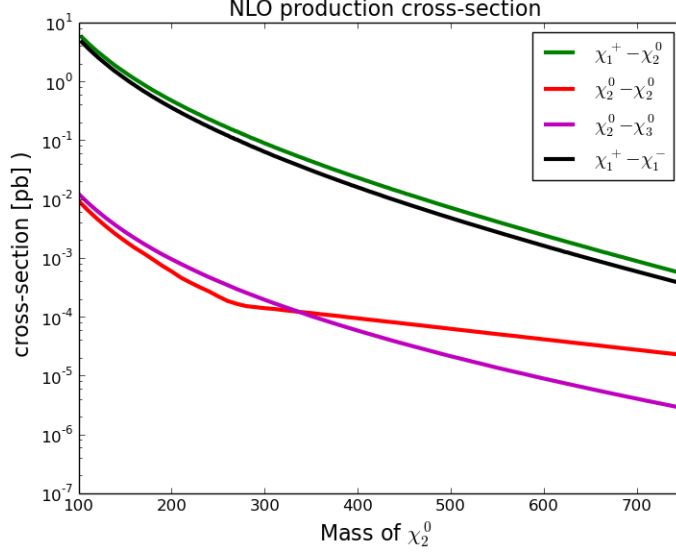
Figure 4.1: Direct production cross-section for channels involving a wino like $\widetilde{\chi}_2^0$ with $m_{\widetilde{\chi}_2^0} = m_{\widetilde{\chi}_1}$. Particle spectrum was generated using SUSEFLAV [25] and cross-section is calculated using Prospino2.1 [26] at an LHC energy of 14 TeV.

greater than any direct electrowino production channel and for heavier electrowino, the $\sigma \times$ BR for $\widetilde{\chi}_2^0$ production via squarks is usually better than the direct production mode. There is another channel which can give LFV signature:

$$\widetilde{\chi}_2^0 \widetilde{\chi}_2^0 \rightarrow l_i^{\pm} l_i^{\pm} l_j^{\mp} l_j^{\mp} \qquad (i \neq j)$$

The channel has a very distict LFV signal comprising of a pair of same sign same flavour leptons. Since it requires flavour violation in the decays of both the neutralinos, the probability of this final state is reduced significantly ($\propto (BR(\widetilde{l}_i \rightarrow l_j)^2)$. Moreover, the cross-section for $\widetilde{\chi}_2^0 \ \widetilde{\chi}_2^0$ pair-production is rather small compared to other electroweakino production channels as can be seen from Fig. (4.1). Despite that, the fact that $l_i^{\pm} l_i^{\pm} l_j^{\mp} l_j^{\mp}$ signal has almost no direct SM background, reduces the total background to the signal appreciably. Clearly there is a trade-off between diminished signal and reduced background and makes it an interesting channel to investigate for the case of LHC running at 14 TeV and at an integrated luminosity of 3000 fb^{-1}.

4.1   Production Cross section

To study the signals of Lepton flavour violation in neutralino decay at the LHC, one needs significant LFV branching fraction. As we have seen, the flavour violating neutralino decay into electron and muon can be parameterized in terms of a rotating angle θ, which, along with the slepton mass difference, is constrained by the corresponding rare decay of muon. We also saw that if the slepton masses are suffieciently degenrate, then the
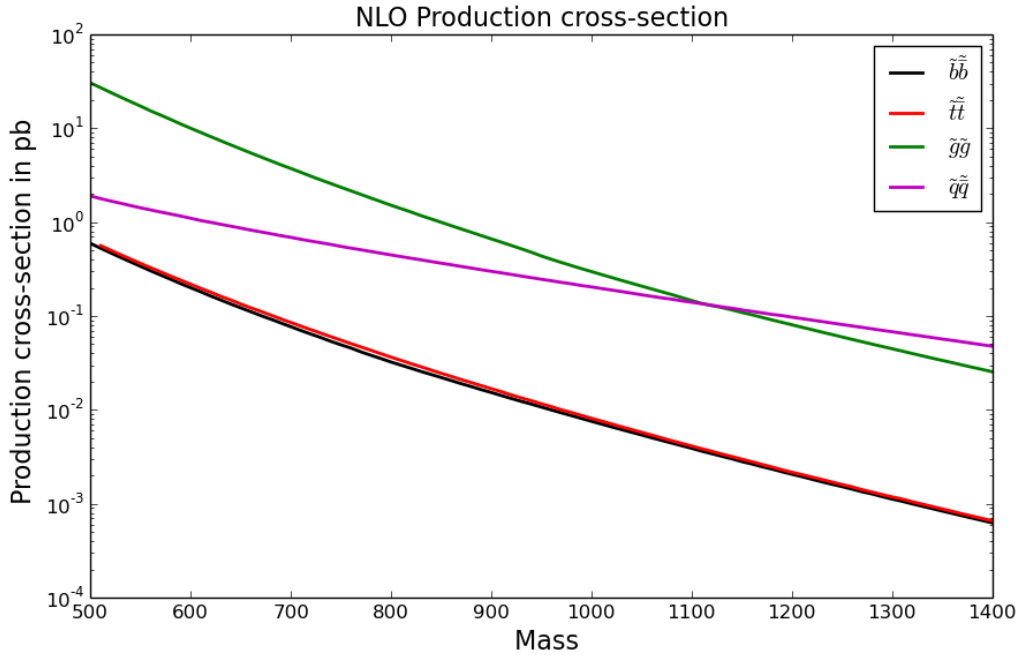
Figure 4.2: Production cross-section for strongly interacting squarks and gluino as a function of their mass calculated using Prospino2.1 and SUSY-HIT at an LHC energy of 14 TeV [27]. In the case of squark pair poduction, gluino mass was set at 2.5 TeV while for gluino pair prosuction, squark masses were taken to be around 1 TeV.

constraint on the angle theta is significantly reduced.

In our analysis, we focus on the 1-2 generation where the final state LFV signal would be $e^{\pm}e^{\pm}\mu^{\mp}\mu^{\mp}$. Similar signal for the 1-3 and 2-3 lepton generation would be marred with the hadronic and leptonic decays of τ which will make extracting the signals difficult and flooded with backgrounds. We carry out the steps assuming flavour mixing angle to be $\theta = \frac{\pi}{6}$. From equation 3.25, for the upper bound on δ_{LL}^{12} of $\sim \mathcal{O}(10^{-5})$ and a slepton mass of around 500 GeV,

$$\Delta m^2 \approx 5.77 \ (GeV)^2 \tag{4.1}$$

In fact, a maximal mixing of $\theta = \frac{\pi}{4}$ can be obtained for $\Delta m^2 \approx 5 \ (GeV)^2$ We take the common slepton mass as 500 GeV. The SUSY spectrum for our model point is generated in pMSSM using SUSY-HIT. The remaining inputs are as follows:

pMSSM parameters			
M_1	425	M_2	550
M_3	2500	μ	800
$\tan\beta$	10	$M_{A_{pole}}$	1000
A_t	0	M_{q1L}	1000
M_{q2L}	1000	M_{q3L}	800
M_{uR}	1000	M_{cR}	1000
M_{tR}	800	M_{dR}	1000
M_{sR}	1000	M_{bR}	800

Table 4.1: pMSSM parameters for LFV analysis

with all the other tri-linear coefficient set to 0. To run SUSY-HIT, the intial input for slepton soft masses were taken as 500 GeV. The degeneracy was specified in the output SLHA file. The spectrum generated is then verified for exclusion using CheckMATE against ATLAS results from ATLAS-CONF-2013-024 [28] (Stop pair production, ATLAS-CONF-2013-047 [29] (inclusive squark pair production), ATLAS-CONF-2013-035 [30] (chargino-neutralino prouction with 3 lepton in final state). These ATLAS analysis were chosen because they have excluded masses which come closest to the spectrum for our model point. From the analysis, we find that the model is not excluded by any of the 3 ATLAS analyses. In fact the minimum β value from among all the signal regions of a single ATLAS analysis were 0.3708 (ATLAS-CONF-2013-047), 0.9448 (ATLAS-CONF-2013-024) and 0.96618 (ATLAS-CONF-2013-035). Since a β value of less than 0.05 implies CLs exclusion at 95 % , the above values, despite being based on LO cross-section, are far from exclusion limit. In short, our model point is not excluded by ATLAS searches and we proceed with it to the next step.

4.2 Number of signal events

For our model point, the following LO cross-sections are obtained using MadGRAPH and SUSY-HIT at 14TeV. The input files required to reproduce these results can be accessed at [31]

Process	σ (fb)
$pp \to \tilde{q}\tilde{q}$	267.8
$pp \to \tilde{q}\bar{\tilde{q}}$	612.1
$pp \to \tilde{q}\tilde{q} \to \chi_2^0\chi_2^0 qq$	11.79
$pp \to \tilde{q}\bar{\tilde{q}} \to \chi_2^0\chi_2^0 qq$	55.66

Now, the relevant χ_2^0 branching ratios are

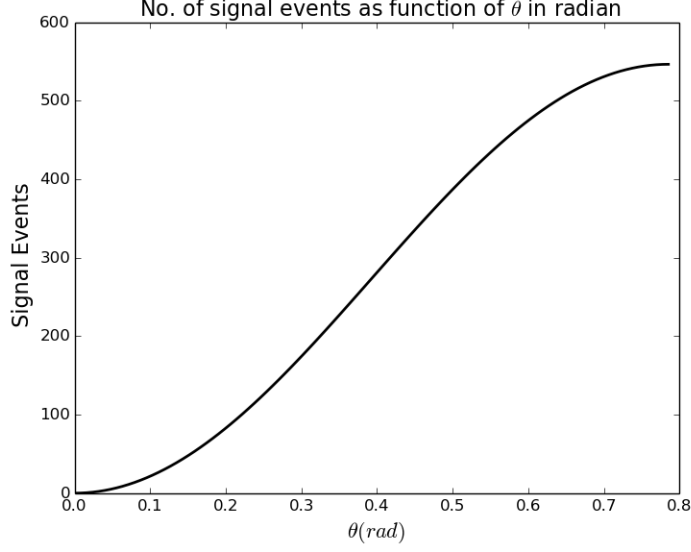$$Br(\tilde{\chi}_2^0 \to e^+e^- \tilde{\chi}_1^0) = 0.1470$$

Figure 4.3: Number of signal events as function of θ in radian for LHC running at $\sqrt{s} = 14$ TeV.

$$Br(\tilde{\chi}_2^0 \to \mu^+ \mu^- \widetilde{\chi}_1^0) \quad = \quad 0.1470 \qquad (4.2)$$

which under LFV mixing gives us

$$Br(\tilde{\chi}_2^0 \to e\mu\widetilde{\chi}_1^0) = 0.0551 \qquad (4.3)$$

and so aur signal rate is given by

$$\chi_2^0\chi_2^0 \to e^+e^+\mu^-\mu^- + \not{E}_T = \sigma_{\chi_2^0\chi_2^0} \times 0.0551 \times 0.0551 \times 0.5 \qquad (4.4)$$

4.3   Background

The background to the signal is extremely small and comes mainly from

- ZZ, $t\bar{t}Z$ decays involving $\tau^+ l_j^- \tau^+ l_j^-$ with both the τ then decaying to l_i^- where $l_k = e, \mu$ and $i \neq j$

- Processes with 2 or 3 leptons and 2 or 1 fake lepton coming from misidentifcation.

The next step would be to analyze the backgound quantitively. Using that one could calculate whether the model point gives a 5σ signal for LFV at the LHC. Further one could do similar analysis for different model points of parameter space and generalize the results for LHC searches.

Chapter 5

Conclusion

In this work, we have studied the implication of constraints coming from lepton flavour violating rare decays $(l_i \rightarrow l_j \gamma)$ on the slepton mass matrix. We have obtained bounds on the off-diagonal elements of slepton mass matrix for the 1-2, 1-3 and 2-3 sector. We found that the off-diagonal elements of 1-2 generation are exteremely constrained $\sim \mathcal{O}(10^{-5})$ by the experimental limit on $\mathrm{Br}(\mu \rightarrow e\gamma)$. The constraints on 1-3 and 2-3 generation are relatively much smaller $\sim \mathcal{O}(10^{-3})$. We also found that for some parameter points there can be cancellations in amplitude for $(l_i \rightarrow l_j\gamma)$ due to which an off-diagonal entry as large as $\sim \mathcal{O}(10^{-1})$ can also be possible (3.1)

The limits on rare decay constrains the off-diagonal elements of slepton mass matrix, which in turn constrains the product of slepton mass splitting and the flavour mixing magnitude. This implies that for sufficiently small mass splittings we can have significant flavour mixing and vice versa. In particular we demanded for the 1-2 generation, a significant flavour mixing angle θ of $\frac{\pi}{6}$ radian, which is possible for a mass insertion parameter δ, of $\sim \mathcal{O}(10^{-5})$ if the slepton mass squared difference is of the order $\sim \mathcal{O}(1)$. With this flavour mixing, we calculated the LFV braching ratio for neutralino and investigated a channel where 2 neutralinos simultaneously undergo LFV decay producing a distinct $e^{\pm}e^{\pm}\mu^{\mp}\mu^{\mp}$ signature which will have a very small background at the LHC. We defined a model in Madgraph with flavour violating interactions and caculated the signal rates for a model point in pMSSM which is not excluded by ATLAS searches. For our particular choice of model point given in Table 4.1, we got more than 500 signal events for a near maximal mixing. In the future, we hope to investigate other regions of the MSSM parameter space for the LFV signal to generalize our results and findings for the LHC phenomenology.

The seacrh for supersymmetric lepton flavour violation in itself is a very interesting and motivated problem in high energy physics. Additionally, SLFV can give rise to another interesting phenomenon called flavored co-annihilation [32] which addresses the problem of excesses in neutralino relic density if χ_1^0 is a dark matter component. In [32], mSUGRA and NUHM models have been studied in details. It would be interesting to revisit and

study the conditions on parameter space and flavor mixing, which could give a neutralino relic density compatible with the experimental limits is obtained.

Appendix A

Searches at The LHC

The Large Hadron Collider (LHC) at CERN has persistantly looked for signals of supersymmetric particles in their searches. As of now, no direct or indirect evidence of supersymmetry has been found. The experiments have served to set exclusion limits on the parameter space of the supersymmetric models. Owing to the great number of parameters in SUSY, the limits are often set in a framework called Simplified Models where specific relation between the participating particles is assumed.

A.1 Simplified Model

A simplified model is defined in terms of particle masses and the related cross sections and branching ratio [33, 34]. For example, the direct production of $\tilde{\chi}_1^{\pm}\tilde{\chi}_1^{\mp}$ with its eventual decay to dilepton along with large missing E_T ($\not{E}$) is dependent on the mass of $\tilde{\chi}_1^{\pm}$, mass of $\tilde{\chi}_1^0$ which appears as $\not{E}$ and the pair production cross section (σ_{pair}). In the simplified approach, the squarks and gluinos are decoupled from the model. For a wino-like $\tilde{\chi}_1^{\pm}$, the cross-section for the process becomes a function of $\tilde{\chi}_1^{\pm}$ mass. The one-step cascade decay brings the mass of intermediate sleptons into consideration, the choice of which alters the kinematics of the analysis. To reduce the dimensionality, slepton mass could be parametrized in terms of chargino and neutralino mass. For instance, in their analysis of this particular channel, CMS[35] and ATLAS[36] took the slepton masses as

$$m_{\tilde{\ell}} = m_{\tilde{\chi}_1^{\pm}} + x(m_{\tilde{\chi}_1^0} - m_{\tilde{\chi}_1^{\pm}}) \tag{A.1}$$

where $0 < x < 1$ and assuming 100% branching fraction. The common choices for x were 0.05, 0.5 and 0.95 .

A.2 Confidence Level:

The $\sigma \times$ BR (for a channel like chargino pair production) is a function of mass and composition/mixing of participating particle [37]. For a given composition, the cross-section usually decreases with mass. The expected number of events for a given process is given by

$$N = \sigma \times Luminosity \times Acceptance \times Efficiency \qquad (A.2)$$

where σ comes from theory while Luminosity, Acceptance and Efficiency depends on the experimental setup.

Since no events in access of that given by SM has been observed at LHC, the null results are used to set upper limits on allowed particle masses. Limits calculated with the CLs method [38, 39] are based on the sampling distribution of the statistic

$$\mathcal{Q} = \prod_{i=1}^{M} \frac{\exp[(-s_i + b_i)](s_i + b_i)^{n_i}}{\exp(-b_i)b_i^{n_i}} \qquad (A.3)$$

or its logarithm

$$q = \ln Q \qquad (A.4)$$

under the signal plus background and background only hypotheses, S and B, respectively. The index i runs over channels, where $s_i = L\sigma$ where L is acceptance times efficiency times integrated luminosity, b_i is the expectation of backgraound and n_i is the number of events observed in the ith channel Given the distributions $p(Q|S)$ and $p(Q|B)$ one calculates a CL_s limit, at level β , by solving the following

$$\beta = \frac{\sum_{Q < Q_0} p(Q|S)}{\sum_{Q < Q_0} p(Q|B)} \qquad (A.5)$$

for the upper limit on the cross-section σ, where q_0 is the observed value of the statistic q. A a cross-section is exclded at 95% if the value of β is less than 0.05

A.3 Testing Model points against data:

The fact that these exclusion limits are obtained under simplyfying assumptions means that the low energy scale has not been excluded exhaustively. Both CMS and ATLAS have performed numerous analyses using different search channels. In order to test whether a model point[1] is excluded or not by a given analysis, one needs to know

- The expected number of signal

---

[1]By model point we mean a specific point in the multi-dimensional parameter space of any of the supersymmetric model like mSUGRA, pMSSM etc.
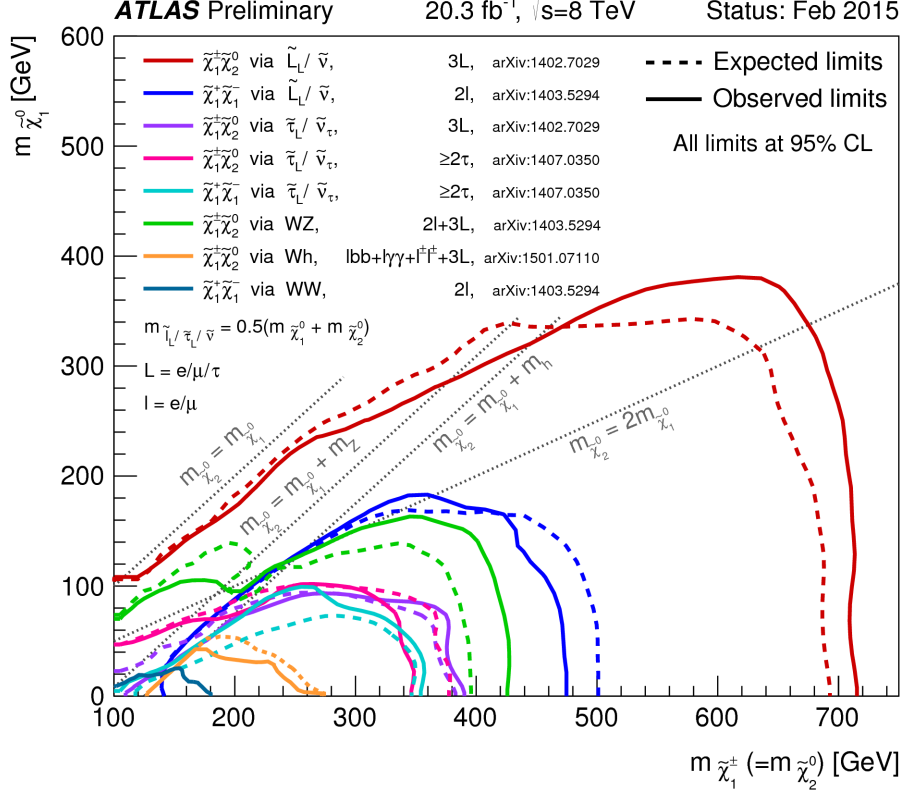
Figure A.1: Exclusion limit for Electroweak chargino and neutralino production by AT-LAS

- The expected signal background

- The actual number of signature events observed

Where the events are defined in terms of final state particles. For instance in [36], the event is defined to comprise of 2 electrons and no jets with high $\not{E}$ and is sensitive to direct slepton pair production and chargino pair production with eventual decay to charged leptons via slepton or W. To improve the signal to background ratio, signal regions are defined using selection cuts on particle momentum(p_T), $\not{E}$ and dilepton invariant mass. In other words, the number of signature events produced and the number taken into account for analysis after imposing selection cuts is different. This reflects in a reduced value of acceptance.

The first step in testing a model point is to obtain the acceptance of the signal region after applying event selection cuts. CheckMATE [40] is a publicly available HEP package which does this job efficiently. The program takes simulated event from event generators like Madgraph [41] and PYTHIA [42] and performs detector simulation using Delphes [43, 44, 45]. The output from Delphes is taken and event selection cuts from the particular analysis of interest are applied. After the selection cuts are applied, the

accepatance changes and is given by

$$Acceptance = \frac{\text{Number of Events before selection cut}}{\text{Number of Events after selection cut}} \qquad (A.6)$$

One must note that this acceptance is not the one dependant on the experimental setup at LHC. This arises because we impose selection requirements on the events with the intention of reducing background. Using this acceptance, the number of expected signal events is normalized

$$N_{Normalized} = \sigma \times Luminosity \times Acceptance \qquad (A.7)$$

Once we have the normalized signal events and the data from LHC analysis, the CLs prescription can be used to find whether a model point is exluded or allowed. CheckMATE does the acceptance calculation and using the prestored data from various ATLAS and CMS analyses, performs the CLs caculation as well. The following is a result reproduced using CheckMATE.
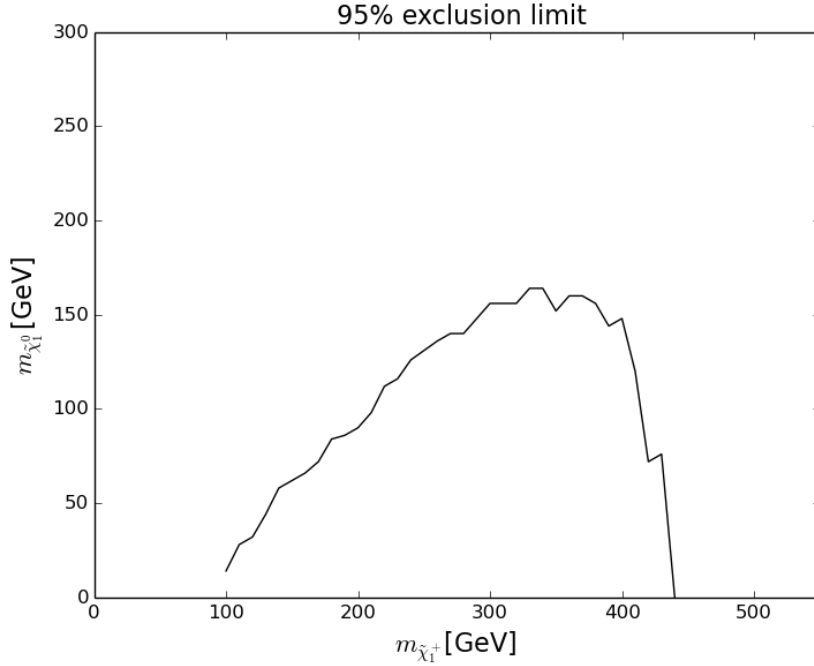

Figure A.2: Exclusion limit for $m_{\tilde{\chi}_1^+}$ in chargino pair production channel with decay to slepton.

A.4 Program for Full BR($l_i \to l_j\gamma$) Calculation

The code is based on formula given in [17, 18]

```python
import numpy as np
import random
import math
generation = int(raw_input("Enter generation as 12 or 13 or 23"))
LeftRight = raw_input("Enter LL or LR or RR")
length = int(raw_input("Enter number of scan iteration")
cos_square_theta = 0.76          # cosine squre of weinberg angle
sin_square_theta = 0.24          # sine square of weinberg angle
tan_theta_weinberg = np.sqrt(0.24/0.76)
MZ = 91.1                        # mass of Z boson
MW = 80.0                        # mass of W boson
mass_tau = 1.777
mass_muon = 0.1056
mass_electron = 0.51/1000
mass = [mass_electron,mass_muon,mass_tau]
Gf= 1.1665651183618914e-05       # fermi constant
alpha=1/137.0


def func1(a):
    return (( 1 - 6*a + 3*a*a + 2*a*a*a -6*a*a*np.log(a))/(6*(1-a)**4))


def func2(a):
    return ((1 - a*a + 2*a*np.log(a))/(1-a)**3)


def func3(a):
    return ((2 + 3*a -6*a*a + a*a*a + 6*a*np.log(a))/(6*(1 - a)**4))



def func4(a):
    return ((-3 + 4*a - a*a - 2*np.log(a))/(1 - a)**3)
br=[]
Delta=[]
M1_array=[]
M2_array=[]
mu_array=[]
selectron_mass_left_array=[]
```

```python
smuon_mass_left_array=[]
stau_mass_left_array=[]
selectron_mass_right_array=[]
smuon_mass_right_array=[]
stau_mass_right_array=[]
file1=open('data_scan_LL_23.out','a')


for loop in range(10000):
    selectron_mass_left = float(random.randint(200,500))
    smuon_mass_left = float(random.randint(200,500))
    stau_mass_left = float(random.randint(200,500))
    selectron_mass_right = float(random.randint(200,500))
    smuon_mass_right = float(random.randint(200,500))
    stau_mass_right = float(random.randint(200,500))
    A_electron = 0.0
    A_muon = 0.0
    A_tau = 000.0
    M1 = float(random.randint(40,600))
    M2 = float(random.randint(103,600))
    mu = float(random.randint(100,1000))
    delta = ((delta_avg + ( 1 - 2*random.random())*delta_diff))
    tanb = float(random.randint(10,30))
    beta = math.atan(tanb)        # beta in radian
    add_left_slepton = (-0.5 + sin_square_theta)*MZ*MZ*np.cos(2*beta)
    add_right_slepton = -(sin_square_theta)*MZ*MZ*np.cos(2*beta)
    add_sneutrino = 0.5*MZ*MZ*np.cos(2*beta)
    i = (generation/10) - 1
    j = (generation%10) - 1
    aa = 0.0
    bb = 0.0
    cc = 0.0
    dd = 0.0
    ee = 0.0
    ff = 0.0
    gg = 0.0
    hh = 0.0
    ii = 0.0
    limit = 0.0
    if (LeftRight == "LL"):
```

```
        if generation == 12:
            aa = delta*selectron_mass_left*smuon_mass_left
            limit = 5.7E-13



        elif generation == 13:
            bb = delta*selectron_mass_left*stau_mass_left


            limit = 3.3E-08


        elif generation == 23:
            ee = delta*smuon_mass_left*stau_mass_left
            limit = 4.4E-08



    elif LeftRight == "LR" or LeftRight =="RL":
        if generation == 12:
            cc = delta*selectron_mass_left*smuon_mass_right
            limit = 5.7E-13



        elif generation == 13:
            dd = delta*selectron_mass_left*stau_mass_right


            limit = 3.3E-08


        elif generation == 23:
            ff = delta*smuon_mass_left*stau_mass_right
            limit = 4.4E-08



    elif LeftRight == "RR":
        if generation == 12:
            gg = delta*selectron_mass_right*smuon_mass_right
            limit = 5.7E-13


        elif generation == 13:
            limit = 3.3E-08
```

```
                  hh = delta*selectron_mass_right*stau_mass_right
          elif generation == 23:
              ii = delta*smuon_mass_right*stau_mass_right
              limit = 4.4E-08




m_selectron_left_square = selectron_mass_left**2
m_smuon_left_square = smuon_mass_left**2
m_stau_left_square = stau_mass_left**2
m_selectron_right_square = selectron_mass_right**2
m_smuon_right_square = smuon_mass_right**2
m_stau_right_square = stau_mass_right**2




CM = np.array([[M2,np.sqrt(2)*MW*np.cos(beta)],[np.sqrt(2)*MW*np.sin(beta),mu]])
CMT = np.transpose(CM)
C=np.dot(CM,CMT)
D, U_star_inv = np.linalg.eig(C)
U_star = np.linalg.inv(U_star_inv)
OR = U_star

CC = np.dot(CMT,CM)
D, V_inv = np.linalg.eig(CC)
OLT = V_inv
OL = np.transpose(OLT)
chargino_mass_matrix = np.dot(OR,np.dot(CM,OLT))
chargino_mass = [chargino_mass_matrix[0][0],chargino_mass_matrix[1][1]]

MN = [[M1,0,-MZ*np.sqrt(sin_square_theta)*math.cos(beta),
MZ*np.sqrt(sin_square_theta)*math.sin(beta)],
[0,M2,MZ*np.sqrt(cos_square_theta)*math.cos(beta),
-MZ*np.sqrt(cos_square_theta)*np.sin(beta)],
[-MZ*np.sqrt(sin_square_theta)*math.cos(beta),
MZ*np.sqrt(cos_square_theta)*math.cos(beta),0,-mu],
[MZ*np.sqrt(sin_square_theta)*math.sin(beta),
-MZ*np.sqrt(cos_square_theta)*np.sin(beta),-mu,0]]

neutralino_mass_matrix,ONT = np.linalg.eig(MN)
```

```python
ON = np.transpose(ONT)
neutralino_mass = [neutralino_mass_matrix[0],neutralino_mass_matrix[1],
neutralino_mass_matrix[2],neutralino_mass_matrix[3]]


Ni_L = [[0.0,0.0,0.0,0.0,0.0,0.0],[0.0,0.0,0.0,0.0,0.0,0.0],
[0.0,0.0,0.0,0.0,0.0,0.0],[0.0,0.0,0.0,0.0,0.0,0.0]]
Ni_R = [[0.0,0.0,0.0,0.0,0.0,0.0],[0.0,0.0,0.0,0.0,0.0,0.0],
[0.0,0.0,0.0,0.0,0.0,0.0],[0.0,0.0,0.0,0.0,0.0,0.0]]
Nj_L = [[0.0,0.0,0.0,0.0,0.0,0.0],[0.0,0.0,0.0,0.0,0.0,0.0],
[0.0,0.0,0.0,0.0,0.0,0.0],[0.0,0.0,0.0,0.0,0.0,0.0]]
Nj_R = [[0.0,0.0,0.0,0.0,0.0,0.0],[0.0,0.0,0.0,0.0,0.0,0.0],
[0.0,0.0,0.0,0.0,0.0,0.0],[0.0,0.0,0.0,0.0,0.0,0.0]]
Ci_R = [[0.0,0.0,0.0],[0.0,0.0,0.0],[0.0,0.0,0.0]]
Ci_L = [[0.0,0.0,0.0],[0.0,0.0,0.0],[0.0,0.0,0.0]]
Cj_R = [[0.0,0.0,0.0],[0.0,0.0,0.0],[0.0,0.0,0.0]]
Cj_L = [[0.0,0.0,0.0],[0.0,0.0,0.0],[0.0,0.0,0.0]]



delta_matrix_sneutrino = [[0,aa,bb],[aa,0,ee],[bb,ee,0]]

delta_matrix_slepton = [[0,aa,bb,0,cc,dd],[aa,0,ee,cc,0,ff],
[bb,ee,0,dd,ff,0],[0,cc,dd,0,gg,hh],[cc,0,ff,gg,0,ii],[dd,ff,0,hh,ii,0]]

slepton_mass_matrix = np.array([[m_selectron_left_square +
add_left_slepton,0,0,(A_electron*mass_electron)-
mass_electron*mu*tanb,0,0],[0,m_smuon_left_square +
add_left_slepton,0,0,(A_muon*mass_muon)-
mass_muon*mu*tanb,0],[0,0,m_stau_left_square +
add_left_slepton,0,0,(A_tau*mass_tau)-mass_tau*mu*tanb],
[(A_electron*mass_electron)-mass_electron*mu*tanb,
0,0,m_selectron_right_square + add_right_slepton,0,0],
[0,(A_muon*mass_muon)-mass_muon*mu*tanb,0,0,
m_smuon_right_square + add_right_slepton,0],
[0,0,(A_tau*mass_tau)-mass_tau*mu*tanb,
0,0,m_stau_right_square + add_right_slepton]])
+ delta_matrix_slepton

slepton_mass, slepton_diagonalizer = np.linalg.eig(slepton_mass_matrix)
sneutrino_mass_matrix = np.array([[m_selectron_left_square +
```

```
add_sneutrino,0,0],[0, m_smuon_left_square + add_sneutrino,0],
[0,0,m_stau_left_square + add_sneutrino]])+ delta_matrix_sneutrino

sneutrino_mass, sneutrino_diagonalizer = np.linalg.eig(sneutrino_mass_matrix)

if ( slepton_mass[0] > 40000 and slepton_mass[1] >40000 and
slepton_mass[2] > 40000 and slepton_mass[3] > 40000 and
slepton_mass[4] >40000 and slepton_mass[5] > 40000 and
sneutrino_mass[0] > 0 and sneutrino_mass[1] > 0 and sneutrino_mass[2] > 0):
    slepton_mass = [np.sqrt(abs(slepton_mass[0])),np.sqrt(abs(slepton_mass[1])),
    np.sqrt(abs(slepton_mass[2])),np.sqrt(abs(slepton_mass[3])),
    np.sqrt(abs(slepton_mass[4])),np.sqrt(abs(slepton_mass[5]))]
    sneutrino_mass = [np.sqrt(abs(sneutrino_mass[0])),
    np.sqrt(abs(sneutrino_mass[1])),
    np.sqrt(abs(sneutrino_mass[2]))]
    UL = np.linalg.inv(slepton_diagonalizer)
    UV = np.linalg.inv(sneutrino_diagonalizer)
    g2=0.652
    gcoeff=g2/np.sqrt(2)
    A_n_L = 0.0
    A_n_R = 0.0
    A_c_R = 0.0
    A_c_L = 0.0
    AL = 0.0
    AR = 0.0
    for A in range(4):
        for X in range(6):
            Ni_L[A][X] = -gcoeff*(((mass[i]*ON[A][2]*(UL[X][i]))
            /(MW*np.cos(beta)))+(2*ON[A][0]*tan_theta_weinberg*
            (UL[X][i+3])))

            Ni_R[A][X] = -gcoeff*((-ON[A][1]-ON[A][0]*tan_theta_weinberg)
            *(UL[X][i])+(mass[i]*ON[A][2]*(UL[X][i+3]))/(MW*np.cos(beta)))

            Nj_L[A][X] = -gcoeff*(((mass[j]*ON[A][2]*(UL[X][j]))
            /(MW*np.cos(beta)))+(2*ON[A][0]*tan_theta_weinberg*(UL[X][j+3])))

            Nj_R[A][X] = -gcoeff*((-ON[A][1] -ON[A][0]*tan_theta_weinberg)
            *(UL[X][j])+(mass[j]*ON[A][2]*(UL[X][j+3]))/(MW*np.cos(beta)))
```

```python
            A_n_L = A_n_L + (((Ni_L[A][X]*np.conjugate(Nj_L[A][X])
            + ((Ni_R[A][X]*(Nj_R[A][X])*(mass[i]/mass[j])))*
            func1((neutralino_mass[A]/(slepton_mass[X]))**2)) +
            (Ni_L[A][X]*(Nj_R[A][X])*neutralino_mass[A]*
            func2((neutralino_mass[A]/(slepton_mass[X]))**2)
            /(mass[j])))/(32*np.pi*np.pi*slepton_mass[X]**2))

            A_n_R = A_n_R + (((Ni_R[A][X]*np.conjugate(Nj_R[A][X])
            + ((Ni_L[A][X]*(Nj_L[A][X])*(mass[i]/mass[j])))*
            func1((neutralino_mass[A]/(slepton_mass[X]))**2)) +
            (Ni_R[A][X]*(Nj_L[A][X])*neutralino_mass[A]*
            func2((neutralino_mass[A]/(slepton_mass[X]))**2)
            /(mass[j])))/(32*np.pi*np.pi*slepton_mass[X]**2))

for A in range(2):
    for X in range(3):
        Ci_R[A][X] = -g2*OR[A][0]*(UV[X][i])
        Ci_L[A][X] = g2*mass[i]*OL[A][1]*(UV[X][i])
        /(np.sqrt(2)*MW*np.cos(beta))
        Cj_R[A][X] = -g2*OR[A][0]*(UV[X][j])
        Cj_L[A][X] = g2*mass[j]*OL[A][1]*(UV[X][j])
        /(np.sqrt(2)*MW*np.cos(beta))

        A_c_L = A_c_L + -(((Ci_L[A][X]*(Cj_L[A][X])+
        (Ci_R[A][X]*(Cj_R[A][X])*(mass[i]/mass[j])))*
        func3((chargino_mass[A]/(sneutrino_mass[X]))**2)) +
        (Ci_L[A][X]*(Cj_R[A][X])*chargino_mass[A]
        *func4((chargino_mass[A]/(sneutrino_mass[X]))**2)
        /(mass[j])))/(32*np.pi*np.pi*sneutrino_mass[X]**2)

        A_c_R = A_c_R + -(((Ci_R[A][X]*(Cj_R[A][X]) +
        (Ci_L[A][X]*(Cj_L[A][X])*(mass[i]/mass[j])))*
        func3((chargino_mass[A]/(sneutrino_mass[X]))**2)) +
        (Ci_R[A][X]*(Cj_L[A][X])*chargino_mass[A]*
        func4((chargino_mass[A]/(sneutrino_mass[X]))**2)
        /(mass[j])))/(32*np.pi*np.pi*sneutrino_mass[X]**2)

AL = A_n_L + A_c_L
```

```
            AR = A_n_R + A_c_R
            br.append(((AL)**2 + (AR)**2)*(48*np.pi*np.pi*np.pi*alpha*0.1739)/(Gf*Gf))
            Delta.append(delta)
            print "slepton_mass ",slepton_mass
            print "sneutrino_mass ", sneutrino_mass
            M1_array.append(M1)
            M2_array.append(M2)
            mu_array.append(mu)
            selectron_mass_left_array.append(selectron_mass_left)
            smuon_mass_left_array.append(smuon_mass_left)
            stau_mass_left_array.append(stau_mass_left)
            selectron_mass_right_array.append(selectron_mass_right)
            smuon_mass_right_array.append(smuon_mass_right)
            stau_mass_right_array.append(stau_mass_right)
            file1.write(str(delta) + '\t' + str(br[-1]) + '\t' + str(M1) +
            '\t' + str(M2) + '\t' + str(mu) + '\t' + str(selectron_mass_left)
            + '\t' + str(smuon_mass_left) + '\t' + str(stau_mass_left) + '\t'
            + str(selectron_mass_right) + '\t' + str(smuon_mass_right) + '\t'
            + str(stau_mass_right) + '\n')
        else:
        continue
file1.close()
```

Bibliography

[1] B. Cleveland, T. Daily, J. Davis, Raymond, J. R. Distel, K. Lande, et al., Measurement of the solar electron neutrino flux with the Homestake chlorine detector, Astrophys.J. 496 (1998) 505–526. doi:10.1086/305343.

[2] Y. Fukuda, et al., Evidence for oscillation of atmospheric neutrinos, Phys.Rev.Lett. 81 (1998) 1562–1567. arXiv:hep-ex/9807003, doi:10.1103/PhysRevLett.81.1562.

[3] T. Cheng, L. Li, Gauge theory of elementary particle physics: Problems and solutions.

[4] J. Adam, et al., New constraint on the existence of the $\mu^+ \rightarrow e^+\gamma$ decay, Phys.Rev.Lett. 110 (2013) 201801. arXiv:1303.0754, doi:10.1103/PhysRevLett.110.201801.

[5] B. Aubert, et al., Searches for Lepton Flavor Violation in the Decays tau+- —¿ e+- gamma and tau+- —¿ mu+- gamma, Phys.Rev.Lett. 104 (2010) 021802. arXiv:0908.2381, doi:10.1103/PhysRevLett.104.021802.

[6] A. Masiero, L. Silvestrini, Two lectures on FCNC and CP violation in supersymmetryarXiv:hep-ph/9711401.

[7] M. Drees, R. Godbole, P. Roy, Theory and phenomenology of sparticles: An account of four-dimensional N=1 supersymmetry in high energy physics.

[8] P. Labelle, Supersymmetry demystified.

[9] M. Maggiore, A Modern introduction to quantum field theory.

[10] S. P. Martin, A Supersymmetry primer, Adv.Ser.Direct.High Energy Phys. 21 (2010) 1–153. arXiv:hep-ph/9709356, doi:10.1142/9789814307505_0001.

[11] S. K. Vempati, Introduction to MSSMarXiv:1201.0334.

[12] R. Adam, et al., Planck 2015 results. I. Overview of products and scientific resultsarXiv:1502.01582.

[13] G. Jungman, M. Kamionkowski, K. Griest, Supersymmetric dark matter, Phys.Rept. 267 (1996) 195–373. `arXiv:hep-ph/9506380`, `doi:10.1016/0370-1573(95)00058-5`.

[14] J. Hisano, T. Moroi, K. Tobe, M. Yamaguchi, Lepton flavor violation via right-handed neutrino Yukawa couplings in supersymmetric standard model, Phys.Rev. D53 (1996) 2442–2459. `arXiv:hep-ph/9510309`, `doi:10.1103/PhysRevD.53.2442`.

[15] P. Paradisi, Constraints on SUSY lepton flavor violation by rare processes, JHEP 0510 (2005) 006. `arXiv:hep-ph/0505046`, `doi:10.1088/1126-6708/2005/10/006`.

[16] M. Arana-Catania, S. Heinemeyer, M. Herrero, New Constraints on General Slepton Flavor Mixing, Phys.Rev. D88 (1) (2013) 015026. `arXiv:1304.2783`, `doi:10.1103/PhysRevD.88.015026`.

[17] J. Hisano, D. Nomura, Solar and atmospheric neutrino oscillations and lepton flavor violation in supersymmetric models with the right-handed neutrinos, Phys.Rev. D59 (1999) 116005. `arXiv:hep-ph/9810479`, `doi:10.1103/PhysRevD.59.116005`.

[18] E. Arganda, M. Herrero, A. Teixeira, mu-e conversion in nuclei within the CMSSM seesaw: Universality versus non-universality, JHEP 0710 (2007) 104. `arXiv:0707.2955`, `doi:10.1088/1126-6708/2007/10/104`.

[19] R. M. Godbole, CP violation in 0 and the LHC, Czech.J.Phys. 55 (2005) B221–B231. `arXiv:hep-ph/0503088`, `doi:10.1007/s10582-005-0033-y`.

[20] A. Arbey, J. Ellis, R. Godbole, F. Mahmoudi, Exploring CP Violation in the MSSM, Eur.Phys.J. C75 (2) (2015) 85. `arXiv:1410.4824`, `doi:10.1140/epjc/s10052-015-3294-z`.

[21] K. Olive, et al., Review of Particle Physics, Chin.Phys. C38 (2014) 090001. `doi:10.1088/1674-1137/38/9/090001`.

[22] K. Agashe, M. Graesser, Signals of supersymmetric lepton flavor violation at the CERN LHC, Phys.Rev. D61 (2000) 075008. `arXiv:hep-ph/9904422`, `doi:10.1103/PhysRevD.61.075008`.

[23] J. Hisano, M. M. Nojiri, Y. Shimizu, M. Tanaka, Lepton flavor violation in the left-handed slepton production at future lepton colliders, Phys.Rev. D60 (1999) 055008. `arXiv:hep-ph/9808410`, `doi:10.1103/PhysRevD.60.055008`.

[24] M. Guchait, J. Kalinowski, P. Roy, Supersymmetric lepton flavor violation in a linear collider: The Role of charginos, Eur.Phys.J. C21 (2001) 163–169. `arXiv:hep-ph/0103161`, `doi:10.1007/s100520100727`.

[25] D. Chowdhury, R. Garani, S. K. Vempati, SUSEFLAV: Program for supersymmetric mass spectra with seesaw mechanism and rare lepton flavor violating decays, Comput.Phys.Commun. 184 (2013) 899–918. `arXiv:1109.3551`, `doi:10.1016/j.cpc.2012.10.031`.

[26] W. Beenakker, R. Hopker, M. Spira, PROSPINO: A Program for the production of supersymmetric particles in next-to-leading order QCD`arXiv:hep-ph/9611232`.

[27] A. Djouadi, M. Muhlleitner, M. Spira, Decays of supersymmetric particles: The Program SUSY-HIT (SUspect-SdecaY-Hdecay-InTerface), Acta Phys.Polon. B38 (2007) 635–644. `arXiv:hep-ph/0609292`.

[28] Search for direct production of the top squark in the all-hadronic ttbar + etmiss final state in 21 fb-1 of p-pcollisions at sqrt(s)=8 TeV with the ATLAS detector.

[29] T. A. collaboration, Search for squarks and gluinos with the ATLAS detector in final states with jets and missing transverse momentum and 20.3 fb^{-1} of $\sqrt{s} = 8$ TeV proton-proton collision data.

[30] Search for direct production of charginos and neutralinos in events with three leptons and missing transverse momentum in $21\,\mathrm{fb}^{-1}$ of pp collisions at $\sqrt{s} = 8\,\mathrm{TeV}$ with the ATLAS detector.

[31] Link to relevant files.

[32] D. Choudhury, R. Garani, S. K. Vempati, Flavored Co-annihilations, JHEP 1206 (2012) 014. `arXiv:1104.4467`, `doi:10.1007/JHEP06(2012)014`.

[33] S. Chatrchyan, et al., Interpretation of Searches for Supersymmetry with simplified Models, Phys.Rev. D88 (5) (2013) 052017. `arXiv:1301.2175`, `doi:10.1103/PhysRevD.88.052017`.

[34] D. Alves, et al., Simplified Models for LHC New Physics Searches, J.Phys. G39 (2012) 105005. `arXiv:1105.2838`, `doi:10.1088/0954-3899/39/10/105005`.

[35] V. Khachatryan, et al., Searches for electroweak production of charginos, neutralinos, and sleptons decaying to leptons and W, Z, and Higgs bosons in pp collisions at 8 TeV, Eur.Phys.J. C74 (9) (2014) 3036. `arXiv:1405.7570`, `doi:10.1140/epjc/s10052-014-3036-7`.

[36] G. Aad, et al., Search for direct production of charginos, neutralinos and sleptons in final states with two leptons and missing transverse momentum in *pp* collisions at $\sqrt{s} = 8$ TeV with the ATLAS detector, JHEP 1405 (2014) 071. `arXiv:1403.5294`, `doi:10.1007/JHEP05(2014)071`.

[37] W. Beenakker, M. Klasen, M. Kramer, T. Plehn, M. Spira, et al., The Production of charginos / neutralinos and sleptons at hadron colliders, Phys.Rev.Lett. 83 (1999) 3780–3783. `arXiv:hep-ph/9906298`, `doi:10.1103/PhysRevLett.100.029901,10.1103/PhysRevLett.83.3780`.

[38] T. Junk, Confidence level computation for combining searches with small statistics, Nucl.Instrum.Meth. A434 (1999) 435–443. `arXiv:hep-ex/9902006`, `doi:10.1016/S0168-9002(99)00498-2`.

[39] M. P. J. Linnemann, H. B. Prosper., Calculating Confidence Limits - D Note 4491.

[40] M. Drees, H. Dreiner, D. Schmeier, J. Tattersall, J. S. Kim, CheckMATE: Confronting your Favourite New Physics Model with LHC Data, Comput.Phys.Commun. 187 (2014) 227–265. `arXiv:1312.2591`, `doi:10.1016/j.cpc.2014.10.018`.

[41] J. Alwall, M. Herquet, F. Maltoni, O. Mattelaer, T. Stelzer, MadGraph 5 : Going Beyond, JHEP 1106 (2011) 128. `arXiv:1106.0522`, `doi:10.1007/JHEP06(2011)128`.

[42] T. Sjstrand, S. Ask, J. R. Christiansen, R. Corke, N. Desai, et al., An Introduction to PYTHIA 8.2`arXiv:1410.3012`.

[43] J. de Favereau, et al., DELPHES 3, A modular framework for fast simulation of a generic collider experiment, JHEP 1402 (2014) 057. `arXiv:1307.6346`, `doi:10.1007/JHEP02(2014)057`.

[44] M. Cacciari, G. P. Salam, G. Soyez, FastJet User Manual, Eur.Phys.J. C72 (2012) 1896. `arXiv:1111.6097`, `doi:10.1140/epjc/s10052-012-1896-2`.

[45] M. Cacciari, G. P. Salam, G. Soyez, The Anti-k(t) jet clustering algorithm, JHEP 0804 (2008) 063. `arXiv:0802.1189`, `doi:10.1088/1126-6708/2008/04/063`.